

**ENHANCED OIL RECOVERY BY SURFACTANT-
ENHANCED VOLUMETRIC SWEEP EFFICIENCY**

**First Annual Report for the Period
September 30, 1985-September 30, 1986**

**By
Jeffrey H. Harwell
John F. Scamehorn**

May 1987

Performed Under Contract No. AC19-85BC10845

**University of Oklahoma
Norman, Oklahoma**

**Bartlesville Project Office
U. S. DEPARTMENT OF ENERGY
Bartlesville, Oklahoma**

SCAMEHORN



DISCLAIMER

This report was prepared as an account of work sponsored by an agency of the United States Government. Neither the United States Government nor any agency thereof, nor any of their employees, makes any warranty, express or implied, or assumes any legal liability or responsibility for the accuracy, completeness, or usefulness of any information, apparatus, product, or process disclosed, or represents that its use would not infringe privately owned rights. Reference herein to any specific commercial product, process, or service by trade name, trademark, manufacturer, or otherwise, does not necessarily constitute or imply its endorsement, recommendation, or favoring by the United States Government or any agency thereof. The views and opinions of authors expressed herein do not necessarily state or reflect those of the United States Government or any agency thereof.

Printed in the United States of America. Available from:
National Technical Information Service
U.S. Department of Commerce
5285 Port Royal Road
Springfield, VA 22161

NTIS price codes

Paper copy: **A05**

Microfiche copy: **A01**

**ENHANCED OIL RECOVERY BY
SURFACTANT-ENHANCED VOLUMETRIC SWEEP EFFICIENCY**

**First Annual Report for the Period
September 30, 1985-September 30, 1986**

**By
Jeffrey H. Harwell
John F. Scamehorn**

May 1987

Work Performed Under Contract No. AC19-85BC10845

**Prepared for
U.S. Department of Energy
Assistant Secretary for Fossil Energy**

**Fred W. Burtch, Project Manager
Bartlesville Project Office
P.O. Box 1398
Bartlesville, OK 74005**

**Prepared by
University of Oklahoma
School of Chemical Engineering & Materials Science
Norman, OK 73019**

ABSTRACT

Surfactant-enhanced volumetric sweep efficiency is a novel EOR method which utilizes precipitation/coacervation of surfactants to plug the most permeable regions of the reservoir, improving the efficiency of a waterflooding operation. This technique does not rely on reduction of interfacial tension between aqueous and oleic phases to enhance oil recovery. Therefore, even though surfactants are involved, this new technique is not a substitute or improvement on classical surfactant flooding; however, it has the potential to compete with polymer flooding as an alternative sweep efficiency improvement method.

In surfactant-enhanced volumetric sweep efficiency, a slug containing one kind of surfactant is injected into the reservoir, followed by a brine spacer. This is followed by injection of a second kind of surfactant which has lower adsorption than the first surfactant used. The system is designed so that the chromatographic waves for the two surfactants intersect at a selected distance from the well bore. The surfactants are selected so that they form a precipitate or coacervate when in contact with each other. The resulting precipitate or coacervate plugs the permeable portion of the reservoir through which the water had been flowing. Subsequent water injections will be forced into the less permeable portion of the reservoir, improving sweep efficiency and oil recovery during this modified waterflood.

Anionic and cationic surfactants are one possible combination for this application. These may form either a precipitate or a coacervate upon mixing. Phase boundaries for some specific systems of this type have been determined over a wide range of conditions and a model developed to describe this behavior. Another possibility is the use of nonionic surfactants, which may form coacervate under proper conditions. The adsorption behavior of mixtures of anionic and nonionic surfactants was measured to aid in modeling the chromatographic effects with these surfactants in the reservoir. Studies with sandpacks of different permeabilities in parallel configuration using mixtures of anionic and cationic surfactants have demonstrated the capability of this method to reduce flow rates through a more permeable sandpack more than that through a less permeable sandpack.

TABLE OF CONTENTS

CHAPTER 1	Introduction	1
CHAPTER 2	Precipitation Phenomena in Mixtures of Anionic and Cationic Surfactants in Aqueous Solutions	6
	INTRODUCTION	6
	EXPERIMENTAL	7
	THEORY	8
	RESULTS AND DISCUSSIONS	10
	CONCLUSIONS	19
	REFERENCES	20
CHAPTER 3	Thermodynamics of Adsorption of Surfactant Mixtures on Minerals	34
	INTRODUCTION	34
	THEORY	36
	EXPERIMENTAL	38
	RESULTS AND DISCUSSIONS	39
	OBSERVATIONS AND CONCLUSIONS	43
	REFERENCES	44
CHAPTER 4	Sandpack Studies	56
	EXPERIMENTAL	61
	RESULTS AND DISCUSSIONS	62
	CONCLUSIONS	64
	NOMENCLATURE	65
	REFERENCES	66

ENHANCED OIL RECOVERY

BY

SURFACTANT-ENHANCED VOLUMETRIC SWEEP EFFICIENCY

CHAPTER 1

INTRODUCTION

Nearly 65% of the original oil in place in the average reservoir is not recoverable with conventional waterflooding technology [1]. This problem is due to both the difficulty of distributing injected water throughout the reservoir and the extent to which the oil can be displaced from those portions of the reservoir which are invaded by the injected fluid. Tertiary or enhanced oil recovery (EOR) methods are used to extract this unrecovered petroleum.

The oil recovery efficiency of the waterflooding process (E_R) is represented by Craig [2] as the product of the microscopic oil displacement efficiency (E_D) and the volumetric sweep efficiency (E_V).

$$E_R = E_D E_V \quad [1]$$

E_R is expressed as a fraction of the oil in place at the start of the process. E_D is the ratio of the volume of oil displaced from a unit segment of reservoir contacted by the injected water to the total oil volume found in that segment. E_V is the fraction of total reservoir volume contacted during the displacement process. This representation makes it clear that small improvements in the volumetric sweep efficiency can have large effects on the overall efficiency of a process.

One of the reasons for the poor distribution of injected water that generally occurs in recovery processes is the capillary forces which arise from the high oil/water interfacial tension in the reservoir [1]; this not only reduces the microscopic displacement efficiency but also results in formation of water channels between injection and producing wells. Natural heterogeneities in reservoir rock properties also contribute to low volumetric sweep

efficiencies. There are several approaches that can be taken for improving the volumetric sweep efficiency of a process. One is to reduce the viscosity of all of the fluids in the reservoir, for example by a thermal recovery method such as steam or fire flooding. Another is to increase the relative viscosity of the injected fluid, such as is attempted in a polymer flood.

But all injected fluids have the tendency to flow through the regions of a heterogeneous reservoir least resistant to fluid flow (having the highest permeability), bypassing the lower-permeability zones. Thus, even methods which can improve the microscopic displacement efficiency primarily recover oil only from the higher-permeability zones. After a substantial amount of oil is recovered from these areas, the water-to-oil ratio in the producing wells increases until it is no longer economical to continue the recovery process. It is evident, then, that if a selective plugging method could be developed that would block off those regions of the reservoir preferentially contacted by injected fluid after a substantial portion of the oil in those higher permeability regions had been recovered, so that any subsequently injected fluids would have to pass through the zones that have not been previously contacted, an ultimate increase in both oil-to-water ratios in the producing wells and final recovery of oil-in-place would occur.

Interest in plugging those portions of the reservoir which are preferentially invaded by injected fluids has continually increased over the last forty years so that numerous methods have been proposed to isolate or plug the higher-permeability regions of a reservoir. Among the injection agents currently being investigated are foams, polymers, and microbes [3-6]. But each of these has limited application and faces some problems of varying degrees of severity. Foams, for example, are non-equilibrium structures which may decay too early in the course of an enhanced oil recovery project to have a substantial effect on the overall efficiency of a recovery process. They are also proving difficult to form in situ. Polymers, agents in several processes of current interest, are degraded by shear forces as they are propagated through the reservoir matrix; they are also degraded by microbial action and temperature. Because of their high molecular weight, they also tend to lower injection rates because of the increased viscosity of the injected fluid. In microbial EOR, where cell mass, cell debris and possibly metabolic byproducts of the injected organisms are the blocking agents, the majority of plugging has tended to occur at the inlet end of laboratory cores due to the strong adsorption of the injected bacteria or bacteria spores on the reservoir rock, at least in results reported to date.

The objective of the research presented here is to

examine a novel method for plugging or sealing off the high permeability regions of a reservoir. In this new process two very dilute surfactant slugs (concentrations on the order of hundredths of a weight per cent) are sequentially injected into the formation, with a brine spacer injected between them. As they are injected, the two surfactant solutions have viscosities very little different from brine because they are so dilute. The surfactants are chosen, however, so that 1) the first injected component will have a lower chromatographic velocity in the reservoir than the second and so that 2) upon mixing of the two surfactant solutions in the reservoir, a phase change will occur, resulting in the formation of either a solid precipitate or a viscous, gel-like coacervate phase capable of blocking the region in which mixing occurs. The proposed mechanism depends entirely on the ability of surfactant solutions to undergo equilibrium phase changes when they are mixed. Unlike the attainment of ultralow oil/water interfacial tensions, such phase changes can occur over a wide range of solution parameters, being relatively insensitive to counterion concentrations, temperatures, and make-up of the residual oil. The formation of a solid precipitate or gel-like coacervate which occurs on in situ mixing can partially or completely block the high-permeability zones in which the mixing occurs and divert the fluid flow into new regions of the reservoir which have a higher oil saturation. A larger volume of the reservoir is thus contacted by the injected fluid, improving the overall volumetric sweep efficiency.

There are several potentially major advantages to this new method over other selective permeability reduction techniques studied to date. With the new process proposed here it is possible to control the distance from the injection point at which plugging occurs; that is, the mixing process is delayed until the surfactant solutions are an arbitrary distance away from the well bore and deep into the high permeability areas. The distance from the injection point at which plugging occurs can be controlled mainly because of the different chromatographic velocities at which surfactants travel through the reservoir. Another advantage is that, since formation of precipitate or coacervate is not instantaneous, a relatively thick zone of precipitate or coacervate can form before formation blockage prevents further interpenetration of the two solutions.

Though making use of surfactants, the new process is not to be confused with classical (low tension) surfactant flooding, which is designed to enhance oil recovery by reducing oil/water interfacial tension. The new process introduced here improves oil recovery, not by improving microscopic displacement efficiency, but rather by improving the volumetric sweep efficiency of any secondary or tertiary process by selectively blocking off the high-permeability regions of a reservoir. Since phase separation can occur

with only ppm concentrations of surfactant, the large up-front cost of classical surfactant flooding is potentially avoidable, and injectivities should remain high during the process. Because of the expected greater tolerance for variation in process parameters, the engineering needed for a surfactant enhanced volumetric sweep efficiency process is also potentially much less than a low-tension surfactant flood.

REFERENCES

1. D.O. Shah and R.S. Schechter (eds.), Improved Oil Recovery by Surfactants and Polymer Flooding, Academic Press, New York City, 1977.
2. F.F. Craig, Jr., "Waterflooding," Secondary and Tertiary Oil Recovery Processes, Interstate Oil Compact Commission, Oklahoma City, 1974.
3. S. L. Wellington, "Biopolymer Solution Viscosity Stabilization - Polymer Degradation and Antioxidant Use," Soc. of Petr. Engr. J., 23, (6), 901, 1983.
4. D.N. Meehan, H.B. Crichlow, D.E. Menzie, "A Laboratory Study of Water Immobilization for Improved Oil Recovery", J. Pet. Techn., 205, 1978.
5. G.P. Willhite, D.W. Green, S. Vossoughi, "Evaluation of Reducing Permeability in Porous Rocks by In Situ Polymer Treatments," Contracts for Field Projects and Supporting Research on Enhanced Oil Recovery and Improved Drilling Technology, Progress Review No. 35, DOE/BETC-83/3 p.38, October 1983.
6. G.E. Jenneman, R.M. Knapp, M.J. McInerney, D.E. Menzie, and D.E. Revus, "Experimental Studies of In-Situ Microbial Enhanced Oil Recovery," Soc. Petr. Eng. J., 24, (1), 33, 1984.

CHAPTER 2

PRECIPITATION PHENOMENA IN MIXTURES OF ANIONIC AND CATIONIC SURFACTANTS IN AQUEOUS SOLUTIONS

INTRODUCTION

Considerable work has been done on the interactions between large organic ions with opposite charge in solution. Some of the most important systems include surfactant-dye, surfactant-polymer and anionic-cationic surfactant mixtures. Surfactant-dye interactions are of interest in pharmaceutical applications where many formulations contain dyes for colorants and surfactants for preservation, solubilization and stabilization purposes [1-4]. Surfactant-dye mixtures have also proven useful in several areas of analytical chemistry [5] including determination of the critical micelle concentration for surfactants [6]. Surfactant-polymer systems have been investigated for application in enhanced oil recovery [7-9] and have also found use in hair rinses and conditioners [10-12]. Anionic-cationic surfactant mixtures are also of interest in pharmacy [13] and analytical chemistry [14-17], as well as wastewater treatment [18], textile wetting and detergency [19].

Precipitation is a common phenomenon that can occur in all of the anion-cation mixtures mentioned above, although in most cases precipitation is undesirable because it renders the surfactant ineffective in solution. To understand precipitation in systems such as these, it is necessary to account for processes such as micellization and coacervate formation, which can also occur in solution. In addition, it is important to examine a wide range of anion and cation concentrations so that sufficient information is gathered to provide complete phase boundaries.

To date, the precipitation of anionic surfactant [20-23] and anionic-nonionic surfactant mixtures [24,25] with simple inorganic cations has been successfully modeled. In this paper, the same type of approach will be used to develop a model for the entire precipitation phase boundary of an anionic-cationic mixed surfactant system. The anionic-cationic mixture is the simplest of the systems introduced here because both species are surface active and their solution chemistry is well defined (i.e. mixed micelle formation). In surfactant-dye and surfactant-polymer systems, however, one component is not surface active, so

smaller aggregates [5,26,27] or pseudomicelles [1] may form which may be more difficult to account for. However, it is possible that the model presented here could be modified to include these types of interactions and a very valuable, generalized model would result.

EXPERIMENTAL

Materials.

The anionic surfactant used is sodium dodecylsulfate (NaDS), obtained from Fisher Scientific, which was recrystallized twice from a 50/50 mixture of water and ethanol, then dried under vacuum with low heat. The cationic surfactant is dodecylpyridinium chloride (DPCl) which was received as technical grade from Pfaltz and Bayer. This was recrystallized 3 times from an approximately 80/20 mixture of petroleum ether and ethanol and the crystals were dried under vacuum with low heat. Neither surfactant showed a minimum in surface tension curves and no impurities were observed using High Performance Liquid Chromatography with a conductivity detector. The NaCl (Fisher Certified) was used as received and the water was distilled and deionized.

Methods.

To determine a point on the precipitation phase boundary, a series of solutions were prepared (in 100 ml volumetric flasks) each containing a constant amount of NaDS, 0.15 M added NaCl, and varying amounts of DPCl. Surfactant solutions can remain supersaturated for long periods of time before precipitation is complete [22]; therefore, all solutions were cooled to force precipitation to occur. The solutions were then placed in a water bath at $30.0^\circ \pm 0.1^\circ \text{C}$, shaken periodically, and allowed to equilibrate for at least 4 days before determinations were made. If a solution was outside of the precipitation region, crystals would dissolve so that the solution became isotropic. If crystals remained in solution after equilibration, the initial solution composition was considered to be inside the precipitation region. Using this procedure, the boundary of the precipitation region could be determined and in all cases, for a given NaDS concentration, the concentration of DPCl that determined a point on the boundary was accurate to within 10%.

Several techniques were used to detect the presence of precipitate in solutions. In most cases, the phase boundary can be determined accurately by simple visual inspection. However, at low concentrations, where only a small amount of precipitate forms, it is very difficult to see any crystals. A 4 mW helium neon laser (Spectra Physics) was used to obtain more accurate phase boundaries by passing the beam through a series of solutions. At an observation angle of 90° to the incident beam, scattering of the beam was clearly evident in

some solutions, indicating the presence of small particles [21,28].

Another technique used to determine the location of the phase boundary at low surfactant concentrations was a dodecylsulfate anion selective electrode (Roth Scientific) which responds only to free anionic surfactant ions in solution. When electrode response (relative millivolts) is plotted versus increasing DPCl concentration for a series of solutions with constant NaDS, a break occurs at the lowest DPCl concentration where precipitate is present. Similarly, a UV spectrophotometer (Bausch and Lomb) was used to detect monomeric dodecylpyridinium cations in solution. Therefore, for a series of solutions with constant DPCl and increasing NaDS concentration, a break in the plot of absorbance (at 255 nm) versus NaDS concentration indicated the solution in which precipitation first began to occur. In these experiments, suspended particles must be eliminated because they will cause erroneously high absorbance readings. This is accomplished by centrifuging each solution for 30 minutes and allowing them to reequilibrate at 30° C for 24 hours before absorbance is measured.

Surface tension measurements were used to determine the CMC of each pure surfactant in 0.15 M NaCl by a break in the curve of surface tension versus logarithm of surfactant concentration. A DuNuoy ring tensiometer (Central Scientific) with a platinum-iridium ring was used and all the necessary precautions were taken to maximize accuracy [29]. Solutions were allowed to equilibrate at 30° C until surface tension readings stabilized. Equilibration times ranged from 15 minutes for concentrated solutions to 3.5 hours for dilute solutions.

An elemental analysis of the dodecylpyridinium-dodecylsulfate precipitate was performed by Huffman Laboratories (Wheat Ridge, Colorado). The sample was prepared by filtering crystals from several solutions, washing with cold water to remove excess NaCl, and drying under vacuum with low heat.

THEORY

When small amounts of anionic and cationic surfactants are added to an aqueous solution, they completely dissociate and exist only as ionic monomers. As surfactant concentration is increased, micelles begin to form when the critical micelle concentration (CMC) is reached. If the monomer concentrations of anionic and cationic surfactant exceed the solubility product, precipitate will form. There are two basic equilibria, therefore, that must be considered in solutions of anionic-cationic surfactant mixtures: monomer-micelle equilibrium and monomer-precipitate equilibrium. The schematic diagram in Figure 1 demonstrates this point.

As shown in Figure 1, the anionic and cationic surfactants can be present in three environments: as monomer (unassociated molecules); incorporated in mixed (anionic plus cationic) micelles; and as precipitate. The counterions (Na^+ and Cl^-), which have been excluded from Figure 1 for clarity, can be bound onto the micelle surface or present as unassociated ions in solution.

The formation of precipitate can be represented by:



where DSDP represents the salt that is formed from a 1:1 reaction between dodecylsulfate anion (DS^-) and dodecylpyridinium cation (DP^+) in solution. This reaction can be described by a simple solubility product between the ions:

$$K_{sp} = [\text{DS}^-]_{\text{mon}} [\text{DP}^+]_{\text{mon}} f_{\pm}^2 \quad [1]$$

where K_{sp} is the solubility product, $[\text{DS}^-]_{\text{mon}}$ and $[\text{DP}^+]_{\text{mon}}$ are the anionic and cationic surfactant monomer concentrations, respectively, and f_{\pm} is the activity coefficient in solution. The extended Debye-Huckel equation proposed by Davies (30) is used to estimate f_{\pm} :

$$\log f_{\pm} = -0.5139 |z_+ z_-| \left\{ \frac{I}{1+I} - 0.3I \right\} \quad [2]$$

where I is the ionic strength.

The purpose of the model is to calculate where the precipitation phase boundaries are located, i.e. at which concentrations only an infinitesimal amount of precipitate is present in solution. On the boundary, therefore, all surfactant can be assumed to be present in mixed micelles or as monomer. An overall material balance on each surfactant yields:

$$C_{\text{NaDS}} = [\text{DS}^-]_{\text{mon}} + [\text{DS}^-]_{\text{mic}} \quad [3]$$

$$C_{\text{DPCl}} = [\text{DP}^+]_{\text{mon}} + [\text{DP}^+]_{\text{mic}} \quad [4]$$

where C_{NaDS} and C_{DPCl} represent the total concentration of NaDS and DPCl in solution, respectively, and the concentration of each surfactant in mixed micelles is given by $[\text{DS}^-]_{\text{mic}}$ and $[\text{DP}^+]_{\text{mic}}$.

In order to calculate the monomer concentration of each surfactant, it is necessary to model the monomer-micelle equilibrium. In general, the composition in the monomer will be different than the micellar composition (surfactant-only basis). Regular solution theory has been widely used to model this equilibrium in surfactant mixtures [24,31-35] and will also be used here. By assuming the micelles are a surfactant pseudo-phase and applying regular solution theory:

$$[\text{DS}^-]_{\text{mon}} = X_{\text{DS}} \text{CMC}_{\text{DS}} \exp\left\{ (1-X_{\text{DS}})^2 W/RT \right\} \quad [5]$$

$$[DP^+]_{mon} = (1 - X_{DS}) CMC_{DP} \exp\{(X_{DS})^2 W/RT\} \quad [6]$$

where CMC_{DS} and CMC_{DP} are the CMC values of the pure surfactants, NaDS and DPCl, at the same electrolyte concentration as the mixed surfactant system of interest, W is the interaction parameter, R is the ideal gas constant and T is the absolute temperature. The mole fraction of surfactant in the micelles, X_{DS} (and $X_{DP} = 1 - X_{DS}$), is on a surfactant-only basis so that:

$$X_{DS} = [DS^-]_{mic} / \{[DS^-]_{mic} + [DP^+]_{mic}\} \quad [7]$$

All samples in this study have 0.15 M added NaCl which is assumed to be swamping electrolyte; i.e., counterions (Na^+ and Cl^-) added to solution from the surfactants are negligible compared to the added NaCl. This simplifies the model in that CMC_{DS} and CMC_{DP} can be assumed constant for all solutions. In addition, the fraction of the total counterions bound onto the charged micelles is considered insignificant due to swamping NaCl. Ionic strength calculations, however, do include surfactant concentrations so:

$$I = 0.15 M + C_{NaDS} + C_{DPCl} \quad [8]$$

In general, it may not be possible to use the simplifications allowed by swamping electrolyte, for instance when no NaCl is added. In such systems it would be necessary to model CMC_{DS} and CMC_{DP} as a function of unbound electrolyte [24,34] which would also require an understanding of counterion binding on the mixed anionic-cationic micelles [36,37].

When phase boundaries are determined experimentally, the total concentration of one of the surfactants is an independent variable. So, if C_{NaDS} is set, the dependent variable of interest is the total concentration of DPCl required to cause precipitation. If K_{sp} , W/RT , CMC_{DS} and CMC_{DP} are known, Equations [1-8] can be solved simultaneously for C_{DPCl} , $[DS^-]_{mon}$, $[DP^+]_{mon}$, f_+ , I , X_{DS} , $[DS^-]_{mic}$, and $[DP^+]_{mic}$. Therefore, the model developed here can be used to predict the precipitation phase boundary.

RESULTS AND DISCUSSION

Composition of precipitate.

Elemental analysis of the precipitate formed between NaDS and DPCl in solution is given in Table I. The S/N mole ratio was determined to be 1.0 which confirms a reaction stoichiometry of 1:1; however, it is puzzling that 0.86% Na was found in the precipitate. The Na here is probably not from NaCl left on the crystals because Cl is virtually

absent. At the same time, it does not seem likely that coprecipitation of NaDS is occurring because this would increase the S/N mole ratio. Several other workers have determined the compositions of similar systems and also concluded a 1:1 complex was formed [17,38,39].

Precipitation without micelles present.

At low surfactant concentrations, where micelles are not present, it is possible to determine the solubility product, K_{sp} , from precipitation data. Under these conditions the monomer concentrations in Equation [1] are equal to the respective total concentrations of each surfactant. One can further manipulate Equation [1] to obtain:

$$\log C_{DPC1} = -\log C_{NaDS} + \log (K_{sp}/f_{+}^2) \quad [9]$$

In this region, surfactant concentrations are so low they essentially do not affect ionic strength, because of swamping NaCl, so f_{+} can be considered to have a constant value (0.758). Therefore, from Equation [9], precipitation data should give a straight line with a slope of -1 and from the intercept it is possible to calculate K_{sp} . Experimental results are given in Figure 2 where K_{sp} is calculated to be $2.24 \times 10^{-10} M^2$.

From Figure 2 it is evident that at these very low surfactant concentrations it is not easy to detect the actual location of the precipitation boundary. Visual determination is limited because it is very difficult to see less than $3 \times 10^{-6} M$ formed precipitate. Analytical instruments such as a surfactant selective electrode or UV spectrophotometer are limited because they can not detect surfactant concentrations below approximately $5 \times 10^{-6} M$. Surface tension measurements and laser scattering experiments proved to be the most useful techniques to determine onset of precipitation when visual determination was limited. Although surface tension is usually used to determine formation of micelles (CMC), it can also be used to detect precipitate or coacervate formation [2,40]. Figure 3 shows surface tension as a function of total surfactant concentration in a NaDS-DPC1 mixture when the mole fraction of NaDS is held constant at 0.990 (surfactant-only basis). The concentration at the break in this curve corresponds to a point on the phase boundary shown in Figure 2.

It seems appropriate at this point to mention another reaction that can occur in mixtures of large organic ions with opposite charges: ion pair formation. This can be represented by:

$$K_{ip} = [DS-DP^+]/([DS^-]_{mon}[DP^+]_{mon}) \quad [10]$$

where K_{ip} is the ion pair constant and $DS-DP^+$ represents the ion pair which is considered to be a charged entity (unlike

precipitate) held together by both hydrophobic and electrostatic interactions. Tomlinson [1] has presented ion pair association constants for several systems and a value of 9.61×10^4 (mole fraction basis) can be obtained from data reported by Mitsubishi [41] on the NaDS-DPCl system. Using this number, and by combining Equations [1] and [10], the ion pair concentration, [DS-DP⁺], is calculated to be 4.0×10^{-4} M which should be constant along the entire phase boundary. This value seems too large considering that if this much ion pairing occurred in these solutions, the precipitation boundary would not extend below 4.0×10^{-4} M for either surfactant. However, from Figure 2, the phase boundary is linear to about 2×10^{-4} M and precipitate can be detected down to 1×10^{-4} M NaDS. Therefore, in this study, ion pair formation will be neglected. There is no doubt that ion pairing can take place, however it is probably more important in dye-surfactant systems of opposite charge where pseudomicelles can form.

Supersaturation is also a very important consideration in determining the concentration at which precipitate begins to form [42]. In surfactant systems with inorganic counterions, it has been clearly shown that precipitation boundaries change as a function of time [22]. In mixed surfactant and surfactant-dye systems, observations confirm that solutions can remain clear for long periods of time, even days, before precipitate begins to form [2,17,26,38]. This problem can be avoided if samples are cooled so that precipitate is forced to form (as discussed in the Experimental section) and then solutions are allowed to equilibrate at the temperature of interest. Much of the precipitation and ion pairing work that has been done has neglected to deal with the problem of supersaturation.

Precipitation with micelles present.

The CMCs for the pure surfactants with 0.15 M added NaCl were measured: $CMC_{DS} = 7.7 \times 10^{-4}$ M and $CMC_{DP} = 4.0 \times 10^{-3}$ M. Using the value of K_{DP} determined in Figure 2 and with $W/RT = -8.62$ (which will be discussed later), Equations [1-8] were solved simultaneously to give the calculated phase boundaries with micelles in solution. The results are shown in Figure 4.

From Figure 4 it is evident that as the monomer-precipitate line approaches the CMC of either pure surfactant, drastic changes occur in the solutions. These sharp breaks along the phase boundary correspond to the points where micelles begin to form in solution. From these points, the precipitation boundary extends as two branches; one branch is DPCl-rich and the other is NaDS-rich. Along the DPCl-rich branch of the phase boundary, calculations from the model are very close to the experimental data. However, the calculated precipitation boundary for the NaDS-rich branch shows substantial deviation from experimental measurements, which is no doubt related to coacervate

formation.

Coacervation refers to the formation of small droplets in solution which are rich in surfactant. These coalesce over a period of time so that the original solution separates into two isotropic liquids: one is rich in surfactant and therefore usually viscous, and the other contains little surfactant. Figure 4 shows that in some of the solutions studied here only coacervate forms, while in other solutions both coacervate and precipitate form; i.e. the precipitation boundary lies within the region where coacervate may form. Indeed, in some solutions it is difficult to determine the presence of precipitate due to turbidity caused by coacervate that has not settled out of solution. In addition, there is a narrow range of solution concentrations, close to the precipitation boundary and within the coacervate region, where there seems to be a transition from viscous coacervate to oily precipitate to crystalline precipitate.

Coacervation has been thoroughly investigated in systems similar to the one studied here and it is generally believed to be caused by the growth of micelles to very large sizes [2,43-46]. Interestingly, in a study of micelle aggregation numbers for a mixture of NaDS and dodecyltrimethylammonium chloride (DTAC), the DTAC-rich micelles showed only a moderate increase in size as the precipitation boundary was approached, whereas the NaDS-rich micelles showed a dramatic size increase [47]. This is consistent with the results in Figure 4 where coacervation only occurs along the NaDS-rich branch.

Although coacervation is a very important topic in interactions between large organic ions of opposite charge [1], the focus of the work here will be on precipitation. In order to gain more understanding about the precipitation phase boundary and why it has two branches extending from the monomer-precipitate line, Equations [1],[5], and [6] are combined to give:

$$K_{sp}/f_+^2 = (X_{DS} - X_{DS}^2) CMC_{DS} CMC_{DP} \exp\{[1 - 2(X_{DS} - X_{DS}^2)]W/RT\} \quad [11]$$

Since f_+ is practically constant, and all other parameters are constant, only one value of $X_{DS} - X_{DS}^2$ will satisfy Equation [11]. This means there are two values of X_{DS} (one DPCl-rich and one NaDS-rich) that occur on the precipitation phase boundary where micelles are present and furthermore, if f_+^2 is essentially constant, these values of X_{DS} are constant along each branch. This can be explained in more detail by considering monomer-micelle equilibrium.

The CMC for a mixed surfactant system can be considered as a type of phase boundary between monomer and micelles with specific compositions. Figure 5 shows this boundary for micelle formation along with the monomer-precipitate boundary calculated from Figure 2. Points A and B in Figure 5 show where the monomer-micelle boundary

intersects the monomer-precipitate boundary. These points represent where monomer, micelles and precipitate are in equilibrium. Point C represents a solution on the monomer-micelle boundary that could never exist. Precipitate would form in a sample at this point so that equilibrium concentrations of surfactant remaining in solution will never exceed the monomer-precipitate line and no micelles would remain in solution. Point D represents a solution in which no precipitate will form because the monomer concentrations are below the precipitate line determined by K_{sp} . At concentrations slightly greater than point D, but still below the precipitation line, only monomer and micelles exist in solution. Therefore, for any solution to be on the precipitation phase boundary and contain micelles, it must have the monomer concentrations existing at points A or B and a corresponding micelle mole fraction given by monomer-micelle equilibrium.

For example, at point A the monomer concentrations of each surfactant are equal to the total concentrations since it is on the phase boundary. Therefore, $C_{DPC1} = [DP^+]_{mon} = 3.0 \times 10^{-3} \text{ M}$ and $C_{NaDS} = [DS^-]_{mon} = 1.3 \times 10^{-7} \text{ M}$, which gives a monomer mole fraction (surfactant-only basis) of 4.3×10^{-5} for NaDS at point A. Equation [11] can be solved to show that the corresponding mole fraction in the micelle is $X_{DS} = 0.124$ at this point. These mole fractions are constant along the entire DPC1-rich branch of the precipitation phase boundary in Figure 4 (assuming that the change in ionic strength is negligible).

If C_{DPC1} is increased by $4.5 \times 10^{-4} \text{ M}$ above point A, then to remain on the precipitation phase boundary, C_{NaDS} must be increased $6.4 \times 10^{-5} \text{ M}$ (so $X_{DS} = 0.124$) and all added surfactant forms micelles because the monomer concentrations must remain constant. An increase from $3.0 \times 10^{-3} \text{ M}$ to $3.45 \times 10^{-3} \text{ M}$ is a small change for the total DPC1 concentration as seen in Figure 4, but an increase from $1.3 \times 10^{-7} \text{ M}$ to $6.4 \times 10^{-5} \text{ M}$ is a tremendous jump in the total NaDS concentration. Of course, a similar argument can be made for the NaDS-rich branch of the phase boundary beginning at point B. This accounts for why drastic changes are seen at the two points on the phase boundary when micelles begin to form.

If total DPC1 concentration is increased above the DPC1-rich branch of the phase boundary, and C_{NaDS} is held constant, precipitate cannot form. This is due to a change in micelle composition, from added DPC1, which in turn affects the monomer composition. The monomer concentrations are now below the monomer-precipitate line (represented by point D in Figure 5) so that precipitate cannot form at these surfactant concentrations. Physically speaking, virtually all the NaDS is in mixed micelles so that the NaDS monomer concentration is too low for precipitation to occur. Other authors have explained crossing of phase boundaries as the solubilization of precipitate in micelles. In reality, however, when C_{DPC1} is increased above the DPC1-rich branch

of the phase boundary, precipitate dissolves to form mixed micelles as dictated by monomer-micelle and monomer-precipitate equilibria. As before, a similar explanation applies when the NaDS-rich branch of the phase boundary is exceeded and solutions become clear.

From this fundamental understanding of the precipitation boundary, it is possible to calculate a value for the regular solution theory interaction parameter, W (or W/RT , which is a dimensionless parameter). In most cases, W/RT is determined from independent surface tension experiments, however for this system precipitation occurred at all except extreme mole fractions. At mole fractions of less than 0.003, the surface tension plots gave a wide minimum in all cases, rather than a sharp break, which made it impossible to determine mixture CMCs. However, it is possible to determine W/RT by using points A and B in Figure 5 because they are located on the monomer-micelle boundary. For instance, from Figure 4, point A exists at $C_{DPC1} = [DP^+]_{mon} = 3.0 \times 10^{-3}$ M and $C_{NaDS} = [DS^-]_{mon} = 1.3 \times 10^{-7}$ M. Inserting these numbers into Equations [5] and [6] gives $X_{DS} = 0.130$ and $W/RT = -8.78$. At point B, $[DP^+]_{mon} = 6.5 \times 10^{-7}$ M and $[DS^-]_{mon} = 6.0 \times 10^{-4}$ M which results in $X_{DS} = 0.880$ and $W/RT = -8.45$. Therefore, a value of $W/RT = -8.62$ was used for all model calculations shown in Figure 4.

It should be noted that the absolute value of W/RT determined here is somewhat lower than other reported values for anionic-cationic systems [31,33]. This is probably due to added NaCl which has been shown to reduce the absolute value of W/RT in anionic-nonionic mixtures [24,48], as well as in one anionic-cationic mixture [31] where W/RT went from -18.5 in H_2O to -13.2 in 0.05 M added electrolyte. There is another factor, however, which may be responsible for the discrepancy in reported values of W/RT . From Figure 5, micelles can only exist at monomer mole fractions (surfactant-only basis) of less than 4.3×10^{-5} NaDS (point A) and greater than 0.9989 NaDS (point B) because precipitation occurs at all mole fractions in between. In general, other workers have determined mixture CMCs at mole fractions well between these extremes. Depending on the K_{sp} of the respective systems, then, some previous work may actually have been detecting the monomer-precipitate phase boundary rather than the CMC since it is difficult to see small amounts of formed precipitate. In fact, a good fit can be obtained for precipitation data along the monomer-precipitate boundary when regular solution theory is used with a value of $W/RT = -15.0$. In any case, it is clear that a knowledge of precipitation boundaries is necessary to avoid mistaking precipitation for micelle formation.

Development of empirical model.

Results using regular solution theory have been shown to be insufficient to model the entire phase boundary when coacervation occurs; however, this type of approach could

still be used if there was a way to account for monomer-micelle-coacervate composition equilibrium. To solve this problem, it may be possible to use regular solution theory for the coacervate [49] if the coacervate composition was known and monomer compositions could be measured, perhaps by using ultrafiltration [50]. Another approach might be to use models that have been proposed for coacervate formation [51,52] however they are very complex and require considerable information. In this work, an empirical model is developed which accounts for the effects of coacervate formation on the precipitation phase boundary.

Along each branch of the precipitation boundary the calculated micelle mole fraction, X_{DS} , has been shown to be constant. This is because there are only two monomer compositions where monomer, micelles, and precipitate are in equilibrium so, from regular solution theory, there are two corresponding values of X_{DS} . However, in the vicinity of the calculated NaDS-rich branch, where the model fails, monomer-micelle equilibrium is affected by micelles growing in size and eventual coacervate formation at higher DPCl concentrations. When DPCl concentration is increased until precipitate begins to form, it represents the point where monomer concentrations intersect the monomer-precipitate line (as discussed from Figure 5). For this specific monomer composition there is a corresponding micelle composition and coacervate composition (when present), which should be constant along the entire precipitation boundary. Therefore, the mole fraction of DS^- that is aggregated as micelles and coacervate, X_{DS}^* , can be represented by:

$$X_{DS}^* = [DS^-]_{agg} / \{ [DS^-]_{agg} + [DP^+]_{agg} \} \quad [12]$$

where $[DS^-]_{agg}$ and $[DP^+]_{agg}$ represent the concentrations of each surfactant that are aggregated, either as micelles or coacervate. Strictly speaking, X_{DS}^* is only a constant when 1) the amount of surfactant present in micelles is insignificant compared to the concentration of surfactant in coacervate, and/or 2) the composition in the micelles is approximately the same as the coacervate composition. Both of these conditions would seem to be valid in this case, because of reasons mentioned earlier, so X_{DS}^* can be assumed to be constant.

It is possible to determine the value of X_{DS}^* for each branch of the precipitation boundary using the experimental data in Figure 4. At high concentrations essentially all of the surfactant is present as micelles or coacervate; i.e. the monomer concentrations are negligible so $[DS^-]_{agg} = [DS^-]_{tot}$ and $[DP^+]_{agg} = [DP^+]_{tot}$. Using this fact, with Equation [12] and data in Figure 4, X_{DS}^* is calculated to be 0.107 for the DPCl-rich branch. This is very close to the value of X_{DS} that was calculated using regular solution theory, which is not surprising because Equation [12] reduces to Equation [7] when coacervate is not present. From data for the NaDS-rich branch, X_{DS}^* is found to be 0.620 which compares to 0.876

calculated using regular solution theory.

To be consistent, the material balances (Equations [3] and [4]) should now be written as:

$$C_{NaDS} = [DS^-]_{mon} + [DS^-]_{a00} \quad [13]$$

$$C_{DPCl} = [DP^+]_{mon} + [DP^+]_{a00} \quad [14]$$

By combining Equations [13] and [14] with Equation [12], upon rearrangement it can be shown that:

$$C_{DPCl} = [DP^+]_{mon} + (1 - X_{DS}^*) (C_{NaDS} - [DS^-]_{mon}) / X_{DS}^* \quad [15]$$

This equation, therefore, can model both branches of the precipitation boundary when the appropriate values for X_{DS}^* , $[DS^-]_{mon}$, and $[DP^+]_{mon}$ are used for each branch. The results are shown in Figure 6.

It should be stressed that monomer concentrations used in Equation [15] are taken to be the points where each branch intersects the monomer-precipitate line (points A and B in Figure 5, as discussed earlier). This assumes, however, that monomer concentrations are constant along each branch of the boundary, which may not necessarily be true for the NaDS-rich branch due to micellar growth and coacervation. This is not an important consideration, though, because any error in $[DS^-]_{mon}$ is insignificant compared to C_{NaDS} which is usually a much larger number. Figure 6 shows that Equation [15] fits the data well for each branch of the precipitation boundary (Equation [9] is still used for the monomer-precipitate line). It is interesting to note that the coacervate phase boundary can be described very well when a value of 0.773 is used for X_{DS}^* . Dubin [53] describes a similar result for a surfactant-polymer system where coacervation only occurred within a certain range of mole fractions.

Prediction of total precipitate formed.

With the entire precipitation boundary successfully modeled, it is possible to calculate how much precipitate will form in any mixture of NaDS and DPCl in solution. The concentration of each surfactant remaining in a solution after precipitation will be given by the equilibrium location on the phase boundary. To calculate the path by which a solution reaches the phase boundary, one can write equations that apply at any time during precipitation:

$$C_{NaDS} = [DS^-]_{unr} + [DS^-]_{ppt} \quad [16]$$

$$C_{DPCl} = [DP^+]_{unr} + [DP^+]_{ppt} \quad [17]$$

where $[DS^-]_{unr}$ and $[DP^+]_{unr}$ represent the concentration of each surfactant that is unreacted, and, $[DS^-]_{ppt}$ and $[DP^+]_{ppt}$ are the concentrations of each surfactant that have reacted to form precipitate. Furthermore:

$$[DS^-]_{ppt} = [DP^+]_{ppt} = [DSDP] \quad [18]$$

because the reaction stoichiometry has been shown to be 1:1 (DS⁻:DP⁺). Combining Equations [16-18] gives:

$$C_{NaDS} - C_{DPCl} = [DS^-]_{unr} - [DP^+]_{unr} = D \quad [19]$$

where D is the concentration difference between unreacted surfactants which will be a constant along the entire precipitation pathway. Figure 7 shows curves of constant D superimposed on the precipitation phase boundary. Therefore, for any mixture of NaDS and DPCl inside the precipitation region, as precipitate forms, the solution concentrations will change along a curve of constant D as shown in Figure 7 and equilibrium concentrations of surfactant remaining in solution (after precipitation is complete) are given by the point of intersection between the appropriate concentration difference curve and the phase boundary. These type of curves have also been used in precipitation of anionic surfactants with inorganic cations [21-54].

It is possible to explicitly calculate the amount of precipitate that forms by expanding material balance Equations [13] and [14] to include precipitate:

$$C_{NaDS} = [DS^-]_{mon} + [DS^-]_{agg} + [DSDP] \quad [20]$$

$$C_{DPCl} = [DP^+]_{mon} + [DP^+]_{agg} + [DSDP] \quad [21]$$

These are substituted into Equation [12] to yield:

$$[DSDP] = \frac{X_{DS}^*(C_{DPCl} - [DP^+]_{mon})}{(2X_{DS}^* - 1)} + \frac{(X_{DS}^* - 1)(C_{NaDS} - [DS^-]_{mon})}{(2X_{DS}^* - 1)} \quad [22]$$

which is only valid if there are micelles present after precipitation; i.e. the precipitation pathway intersects either the NaDS-rich or DPCl-rich branch of the phase boundary. If there are no micelles after precipitation then the concentrations of aggregated surfactant in Equations [20] and [21] are zero. These are combined with Equation [1] to give:

$$K_{sp}/f_{+}^2 = (C_{NaDS} - [DSDP])(C_{DPCl} - [DSDP]) \quad [23]$$

Therefore, if $C_{NaDS} - C_{DPCl} = D > 6.0 \times 10^{-4}$ M then Equation [22] can be solved to determine [DSDP] using $X_{DS}^* = 0.620$, $[DS^-]_{mon} = 6.0 \times 10^{-4}$ M, and $[DP^+]_{mon} = 6.5 \times 10^{-7}$ M. Equation [22] is also used when $D < -3.0 \times 10^{-3}$ M where $X_{DS}^* = 0.107$, $[DS^-]_{mon} = 1.3 \times 10^{-7}$ M, and $[DP^+]_{mon} = 3.0 \times 10^{-3}$ M. At all values of D between these, Equation [23] can be used to calculate the amount of precipitate that forms.

Predictions from Equations [22] and [23] for several NaDS-DPCl mixtures are summarized in Table II and experimental results are shown in Figure 8. To determine [DSDP] experimentally, solutions were centrifuged after precipitation and allowed to reequilibrate at 30° C.

Supernatant was removed and diluted to below the monomer-precipitate line and concentrations of DP^+ were determined using a UV spectrophotometer and standard solutions. The amount of precipitate that forms can be obtained from the difference between C_{DPC1} and the measured equilibrium concentration of DP^+ (after precipitation). Table II shows there is good agreement between predicted and measured [DSDP] values.

CONCLUSIONS

Mixtures of NaDS and DPC1 react in solution to form precipitate over a wide range of concentrations. When no micelles are present in solution, this reaction can be modeled by a simple solubility product between the total surfactant concentrations. When micelles are present, monomer concentrations are used in the solubility product expression and the monomer-micelle equilibrium can be described using regular solution theory. From this approach it can be shown that there are only two monomer compositions (one NaDS-rich and one DPC1-rich) where monomer, micelles, and precipitate can exist in equilibrium. Furthermore, these monomer compositions and the corresponding micelle compositions are constant along each branch of the precipitation phase boundary. The model that is developed predicts precipitation data quite well except in the case where coacervate also forms in solution.

To predict precipitation boundaries when coacervate is present, an empirical model is developed based on results from regular solution theory. In this case, the monomer composition where precipitation occurs corresponds to specific micelle and coacervate compositions which should be constant along the precipitation boundary. Using this fact, combined with a material balance for each surfactant, an equation is developed which calculates precipitation boundaries with or without coacervate present. In addition, a simple extension of this approach provides an explicit equation which predicts the amount of precipitate that forms in any NaDS-DPC1 mixture so that the equilibrium surfactant concentrations (after precipitation) can also be determined.

It is hoped that this work can be extended to other mixtures of large organic ions with opposite charge such as surfactant-dye and surfactant-polymer systems. This would require a thorough understanding of surfactant-poor regions where micellization does not occur over a narrow concentration range, if at all. Supersaturation may also prove to be a very important consideration in obtaining phase boundary data for all of these systems but it has not yet been thoroughly investigated.

REFERENCES

1. Tomlinson, E., Davis, S.S., and Mukhayer, G.I., in "Solution Chemistry of Surfactants" (K.L. Mittal, Ed.), Vol. 1, p. 3. Plenum, New York, 1979.
2. Barry, B.W., and Russel, G.F.J., J. Pharm. Sci. **61**, 502 (1972).
3. Attwood, D., and Florence, A.T., "Surfactant Systems", p. 388. Chapman and Hall, New York, 1983.
4. Tomlinson, E., and Davis, S.S., J. Colloid Interface Sci. **66**, 335 (1978).
5. Diaz Garcia, M.E., and Sanz-Medel, A., Talanta **33**, 255 (1986).
6. Mukerjee, P., and Mysels, K.J., J. Am. Chem. Soc. **77**, 2937 (1955).
7. Nagarajan, R., and Harold M.P., in "Solution Behavior of Surfactants" (K.L. Mittal, Ed.), Vol. 2, p. 1391. Plenum, New York, 1980.
8. Sabbadin, J., Le Moigne, J., and Francois, J., in "Surfactants in Solution" (K.L. Mittal, Ed.), Vol. 2, p. 1377. Plenum, New York, 1984.
9. Shah, D.D., and Walker, R.D., "Research on Surfactant-Polymer Oil Recovery Systems", University of Florida, 1980 Annual Report for U.S.DOE Contract No. DE-AC1979BC10075.
10. Great Britian Patent 2,122,898 (1984) [Chem. Abstr. **101**: 12011w].
11. Japan Patent 59,187,095 (1984) [Chem. Abstr. **102**: 190833u].
12. Japan Patent 60,115,511 (1985) [Chem. Abstr. **103**: 220601g].
13. Sadhukhan, B.K., and Chatteraj, D.K., in "Surfactants in Solution" (K.L. Mittal, Ed.), Vol. 2, p. 1249. Plenum, New York, 1984.
14. Zheng, Y., Longdi, L., and Sun, S., Huaxue Tongbao **18**, 16 (1983) [Chem. Abstr. **100**:131587c].
15. Birch, B.J., and Cockroft, R.N., Ion-Sel. Electrode Rev. **3**, 1 (1981).

16. Lin, W., Tang, M., Stranahan, J.J., and Deming, S.N., Anal. Chem. **55**, 1872 (1983).
17. Scowen, R.V., and Leja, J., Can. J. Chem. **45**, 2821 (1967).
18. U.S.S.R. Patent 1,028,605 (1983) [Chem. Abstr. **100**: 12144w].
19. Schwuger, M.J., Kolloid-Z. **243**, 129 (1971).
20. Kallay, N., Pastuovic, M., and Matijevic, E., J. Colloid Interface Sci. **106**, 452 (1985).
21. Matheson, K.L., Cox, M.F., and Smith, D.L., J. Am. Oil Chem. Soc. **62**, 1391 (1985).
22. Peacock, J.M., and Matijevic, E., J. Colloid Interface Sci. **77**, 548 (1980).
23. Celik, M.S., Manev, E.D., and Somasundaran, P., AIChE Symp. Ser. **78**, 86 (1982).
24. Stellner, K.L., and Scamehorn, J.F., J. Am. Oil Chem. Soc. **63**, 566 (1986).
25. Stellner, K.L., and Scamehorn, J.F., "Improving Hardness Tolerance of Anionic Surfactant Solutions by Addition of Nonionic Surfactants", 77th National American Oil Chemist's Society Meeting, Honolulu (May, 1986).
26. Reeves, R.L., and Harkaway, S.A., in "Micellization, Solubilization, and Microemulsions" (K.L. Mittal, Ed.), Vol. 2, p. 819. Plenum, New York, 1977.
27. Burdett, B.C., in "Aggregation Processes in Solution" (E. Wyn-Jones and J. Gormally, Eds.), p. 241. Elsevier Science, New York, 1983.
28. Smith, D.L., Matheson, K.L., and Cox, M.F., J. Am. Oil Chem. Soc. **62**, 1399 (1985).
29. Lunkenheimer, K., and Wantke, K.D., Colloid Polym. Sci. **259**, 354 (1981).
30. Davies, C.W., "Ion Association", p. 41. Butterworths, London, 1962.
31. Rubingh, D.N., in "Solution Chemistry of Surfactants" (K.L. Mittal, Ed.), Vol. 1, p. 337. Plenum, New York, 1979.
32. Holland, P.M., and Rubingh, D.N., J. Phys. Chem. **87**, 1984 (1983).

33. Holland, P.M., Adv. Colloid Interface Sci., in press.
34. Scamehorn, J.F., in "Phenomena in Mixed Surfactant Systems" (J.F. Scamehorn, Ed.), Vol. 311, p. 1. ACS Symp. Ser., ACS, Washington, 1986.
35. Rosen, M.J., and Hua, X.Y., J. Am. Oil Chem. Soc. **59**, 582 (1982).
36. Rathman, J.F., and Scamehorn, J.F., J. Phys Chem. **88**, 5807 (1984).
37. Hall, D.G., and Price, T.J., J. Chem. Soc., Faraday Trans. **80**, 1193 (1984).
38. Hoyer, H.W., and Doerr, I.L., J. Phys. Chem. **68**, 3494 (1964).
39. Nakamura, A., and Muramatsu, M., J. Colloid Interface Sci. **62**, 165 (1977).
40. Goddard, E.D., and Hannan, R.B., J. Colloid Interface Sci. **55**, 73 (1976).
41. Mitsuishi, M., and Hashizume, M., Bull. Chem. Soc. Japan **46**, 1946 (1973).
42. Skoog, D.A., and West, D.M., "Fundamentals of Analytical Chemistry", 2nd Edition, p. 164. Holt, Rhinehart, and Winston, New York, 1969.
43. Mukhayer, G.I., and Davis, S.S., J. Colloid Interface Sci. **66**, 110 (1978).
44. Goodman, J.F., and Walker, T., in "Colloid Science" (D.H. Everett, Ed.), Vol. 3, pp. 230-252. The Chemical Society, London, 1979.
45. Barry, B.W., and Gray, G.M.T., J. Colloid Interface Sci. **52**, 327 (1975).
46. Barry, B.W., and Gray, G.M.T., J. Pharm. Sci. **63**, 548 (1974).
47. Malliaris, A., Binana-Limbele, W., and Zana, R., J. Colloid Interface Sci. **110**, 114 (1986).
48. Hall, D.G., and Huddleston, R.W., Colloids and Surfaces **13**, 209 (1985).
49. Yoesting, D.E., and Scamehorn, J.F., Colloid Polymer Sci. **264**, 148 (1986).
50. Osborne-Lee, I.W., Schechter, R.S., and Wade, W.H., J. Colloid Interface Sci. **94**, 179 (1983).

51. Jokela, P., Jonsson, B., and Wennerstrom, H., Progr. Colloid Polymer Sci. 70, 17 (1985).
52. Jonsson, B., Wennerstrom, H., J. Colloid Interface Sci. 80, 482 (1981).
53. Dubin, P.L., and Davis, D., Colloids and Surfaces 13, 113 (1985).
54. Matheson, K.L., J Am. Oil Chem. Soc. 62, 1269 (1985).

Table I

Analysis of Precipitate Formed Between NaDS
and DPCl in Solution

Element	Calculated ^a	Found
C	67.85	67.81
H	10.71	10.78
O	12.47	12.23
N	2.73	2.72
N (dup.)		2.64
S	6.24	6.08
S (dup.)		6.25
Na	None	0.86
Cl	None	0.11

^a weight percent based on 1:1 complex.

Table II

Comparison between Predicted and Measured
Amounts of DSDP Precipitated

Total Concentration in Solution ^a		Measured Concentrations after Precipitation		Predicted from Model	Path Shown in Figure 8
C_{DPCl}	C_{NaDS}	$[DP^+]_{mon^+}$ $[DP^+]_{agg}$	[DSDP]	[DSDP]	
0.800	1.000	0.004	0.796	0.798	E-E*
1.000	1.000	0.011	0.989	0.980	F-F*
2.000	1.000	0.944	1.056	1.000	G-G*
6.000	5.000	0.744	5.256	5.000	H-H*
4.000	5.000	0.945	3.055	3.367	I-I*
10.000	4.000	6.250	3.750	3.592	J-J*
1.400	1.000	0.331	1.069	0.999	K-K*

^a All concentrations in 10^{-3} moles/liter.

Figure 1. Schematic Diagram of Basic Equilibria in System.

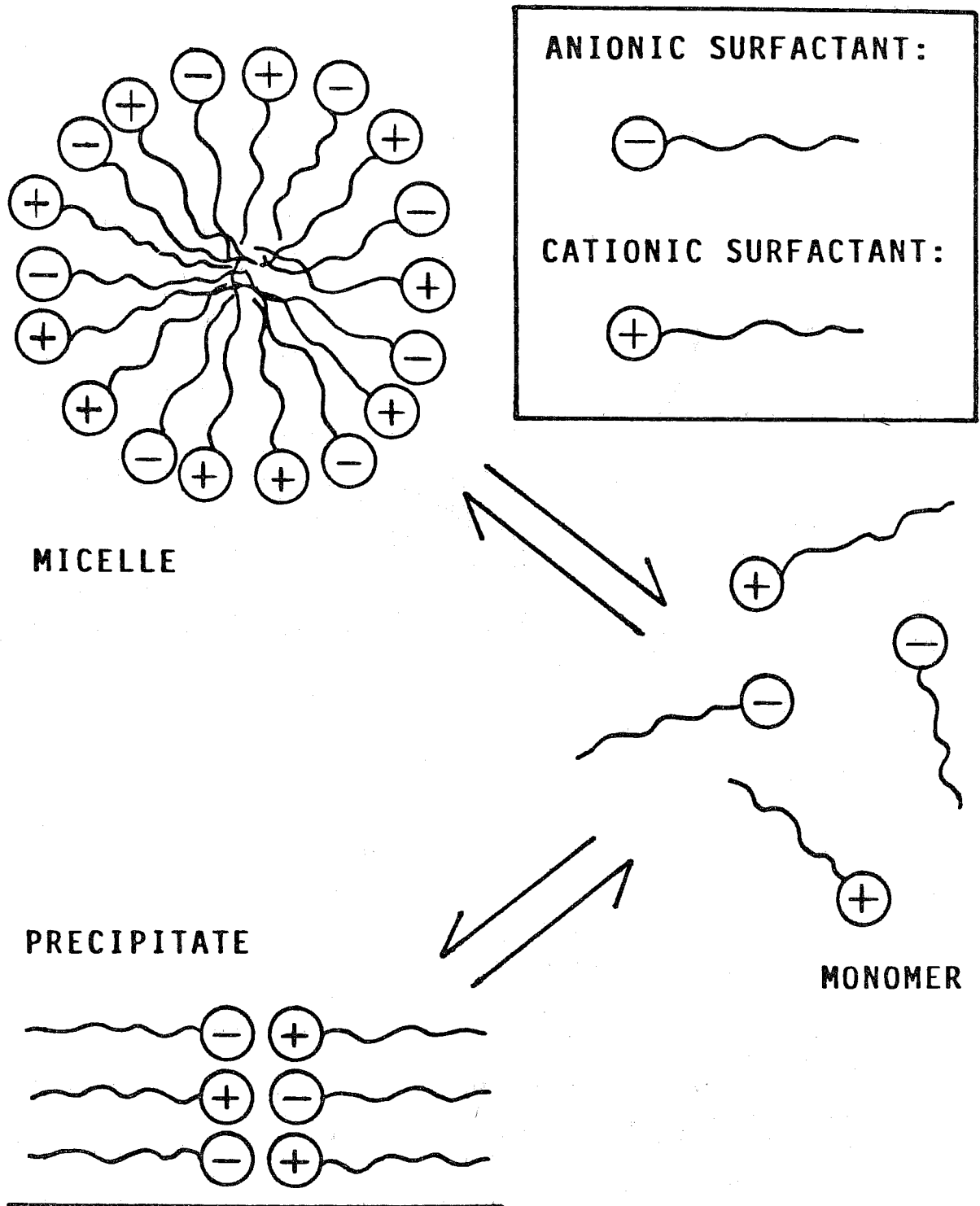


Figure 2. Precipitation Phase Boundary Without Micelles Present.

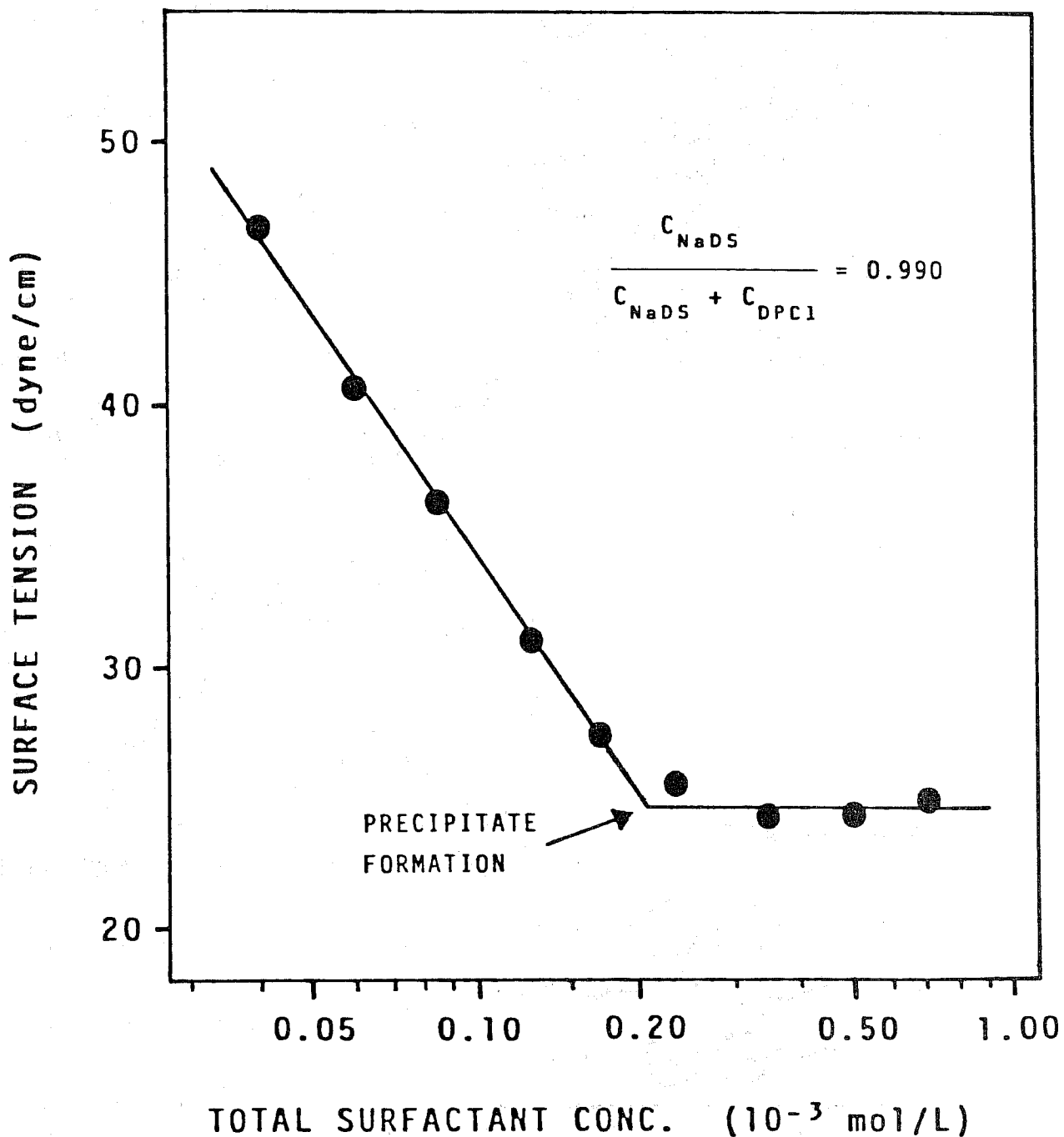


Figure 3. Detection of Precipitate Formation Using Surface Tension Measurements.

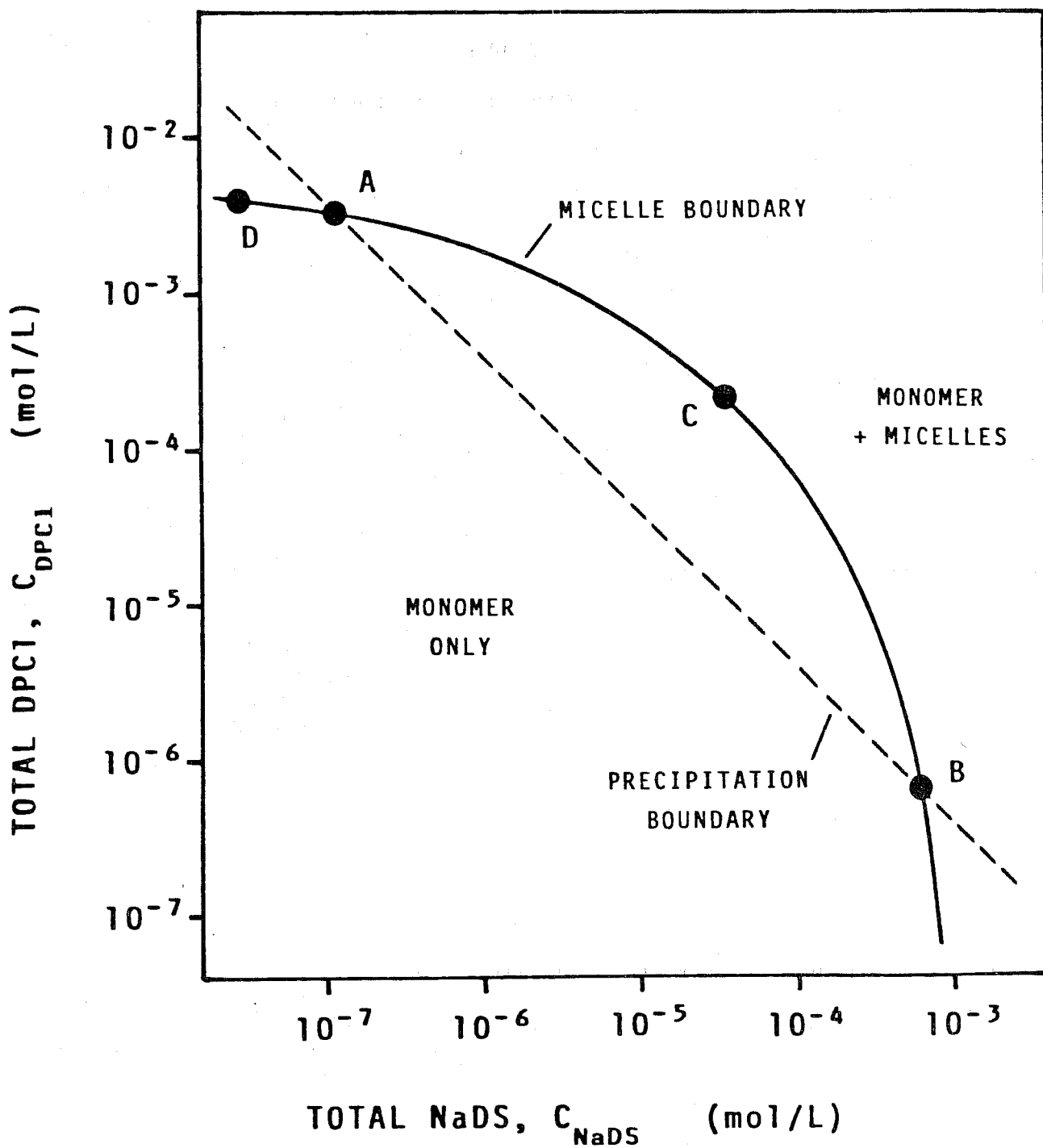


Figure 5. Monomer-Micelle and Monomer-Precipitate Phase Boundaries.

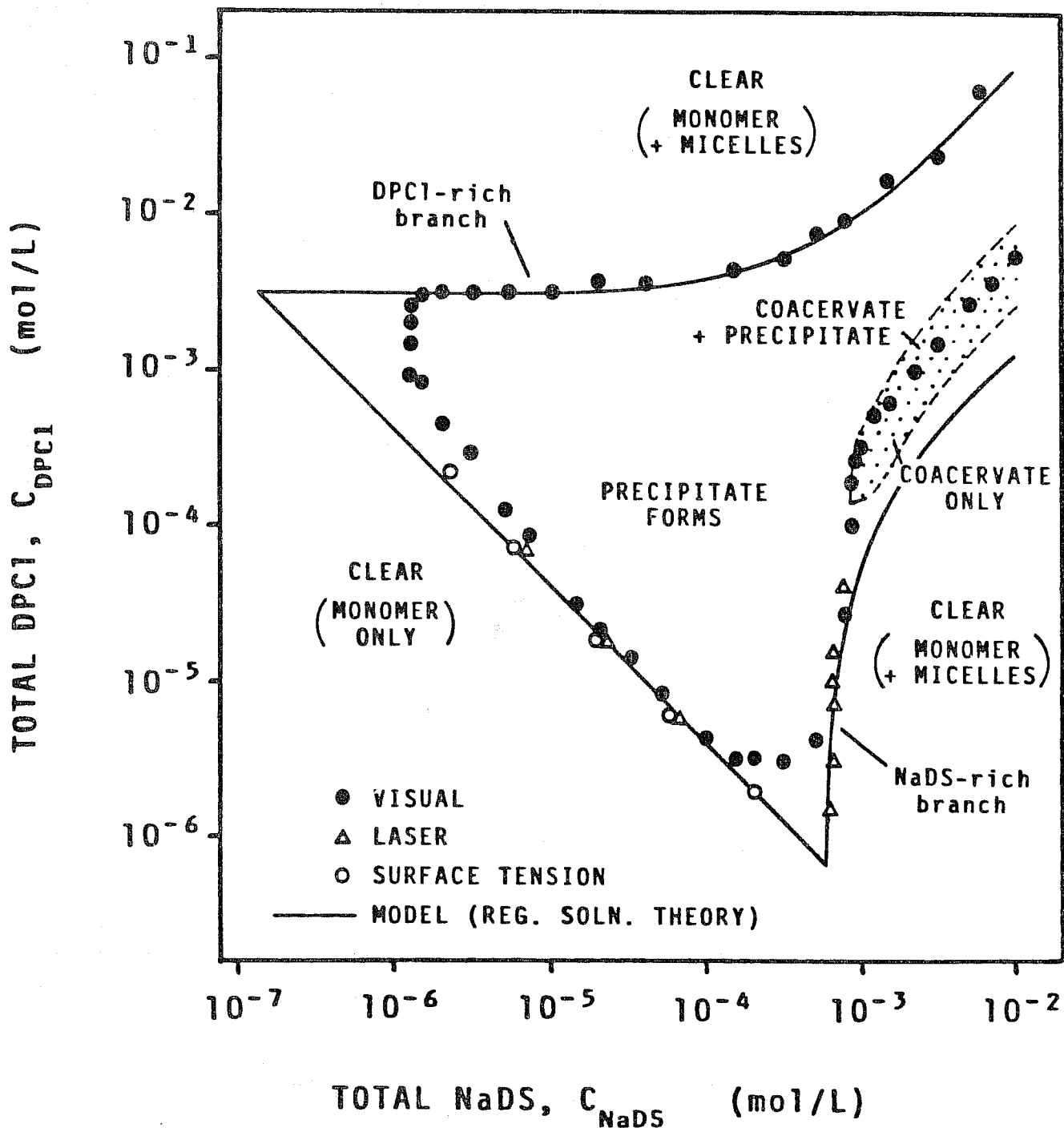


Figure 6. Comparison Between Precipitation Data and Calculations from Empirical Model.

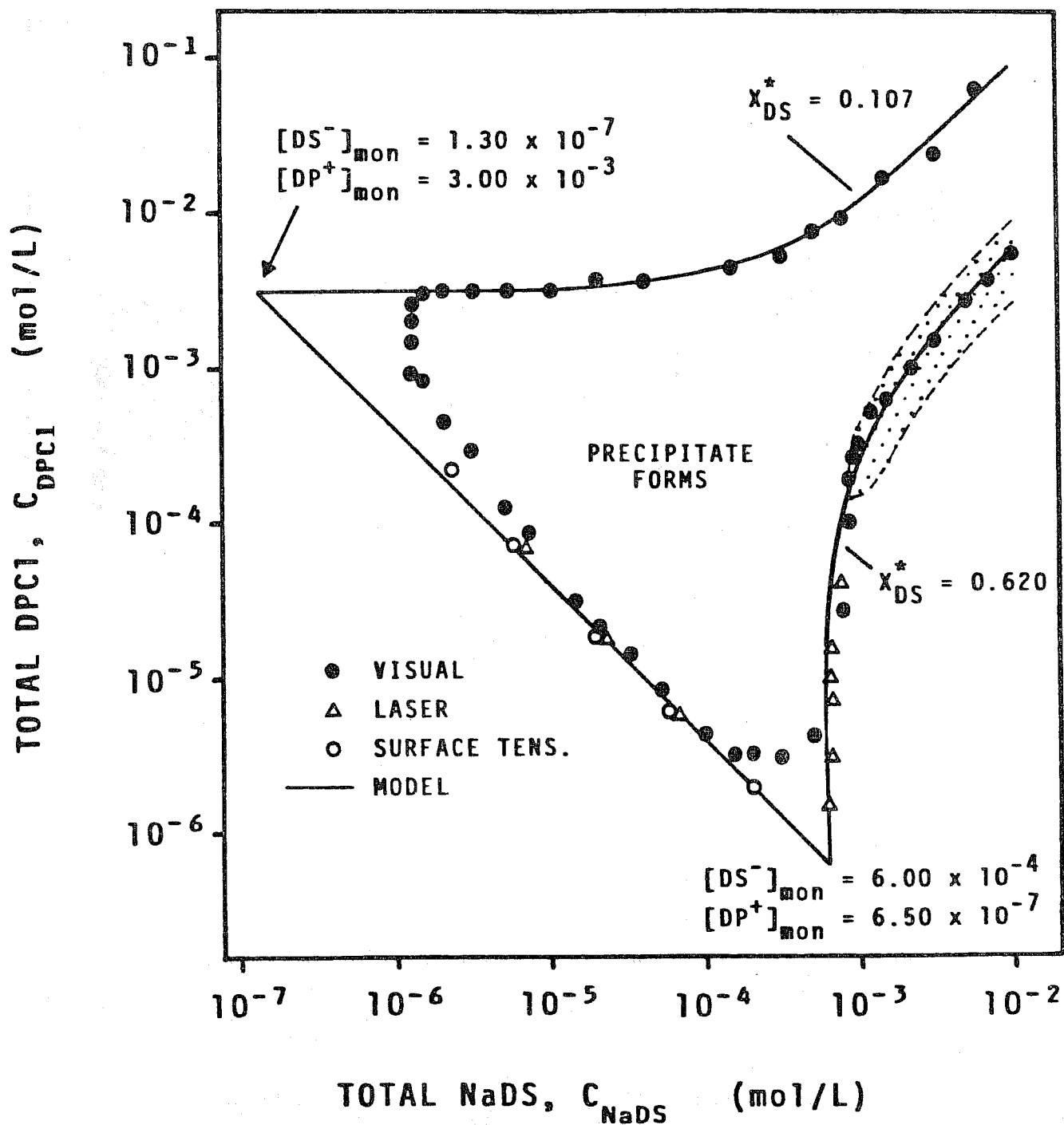


Figure 7. Paths of Precipitate Formation in Relation to the Equilibrium Precipitation Boundary.

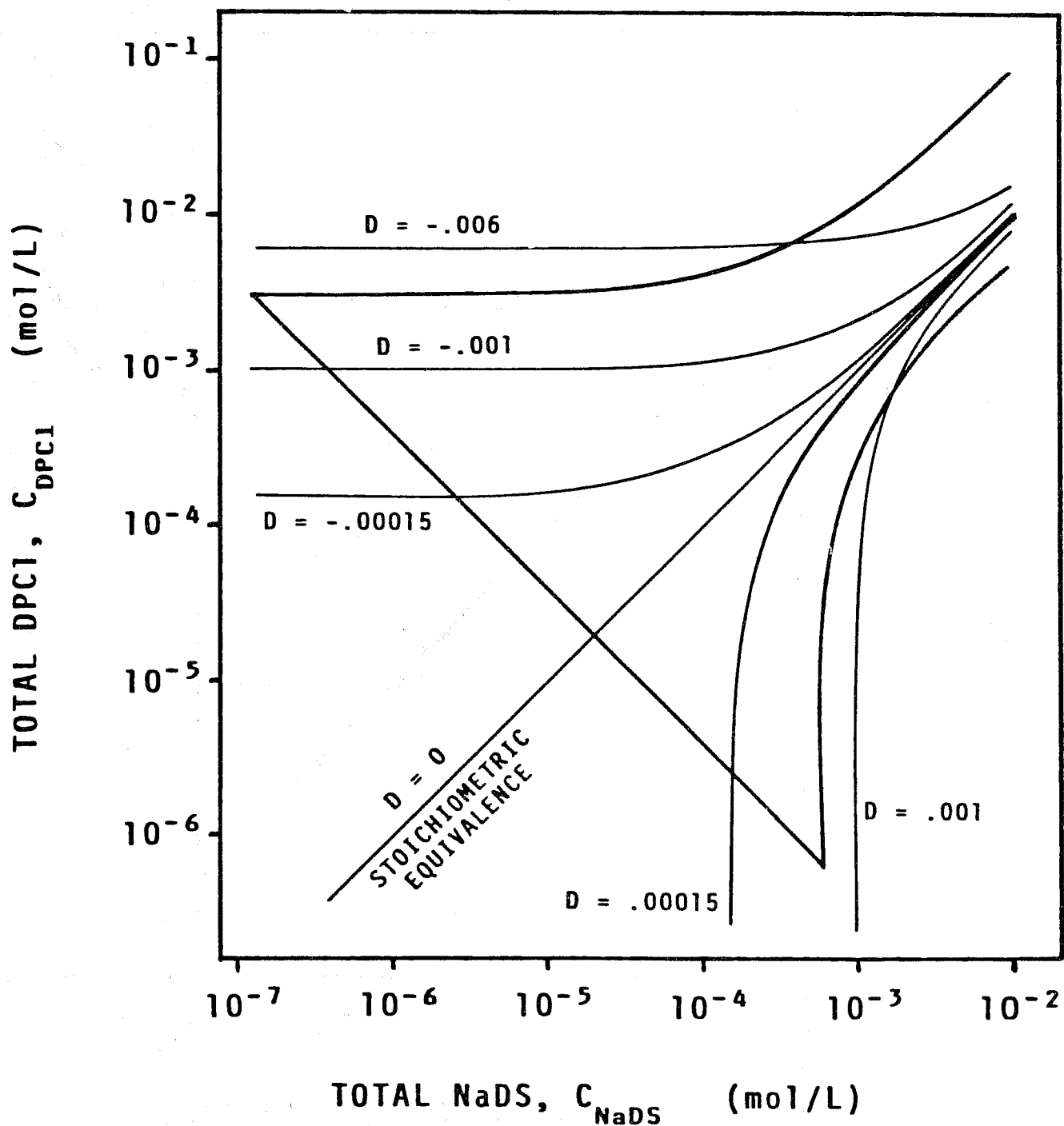
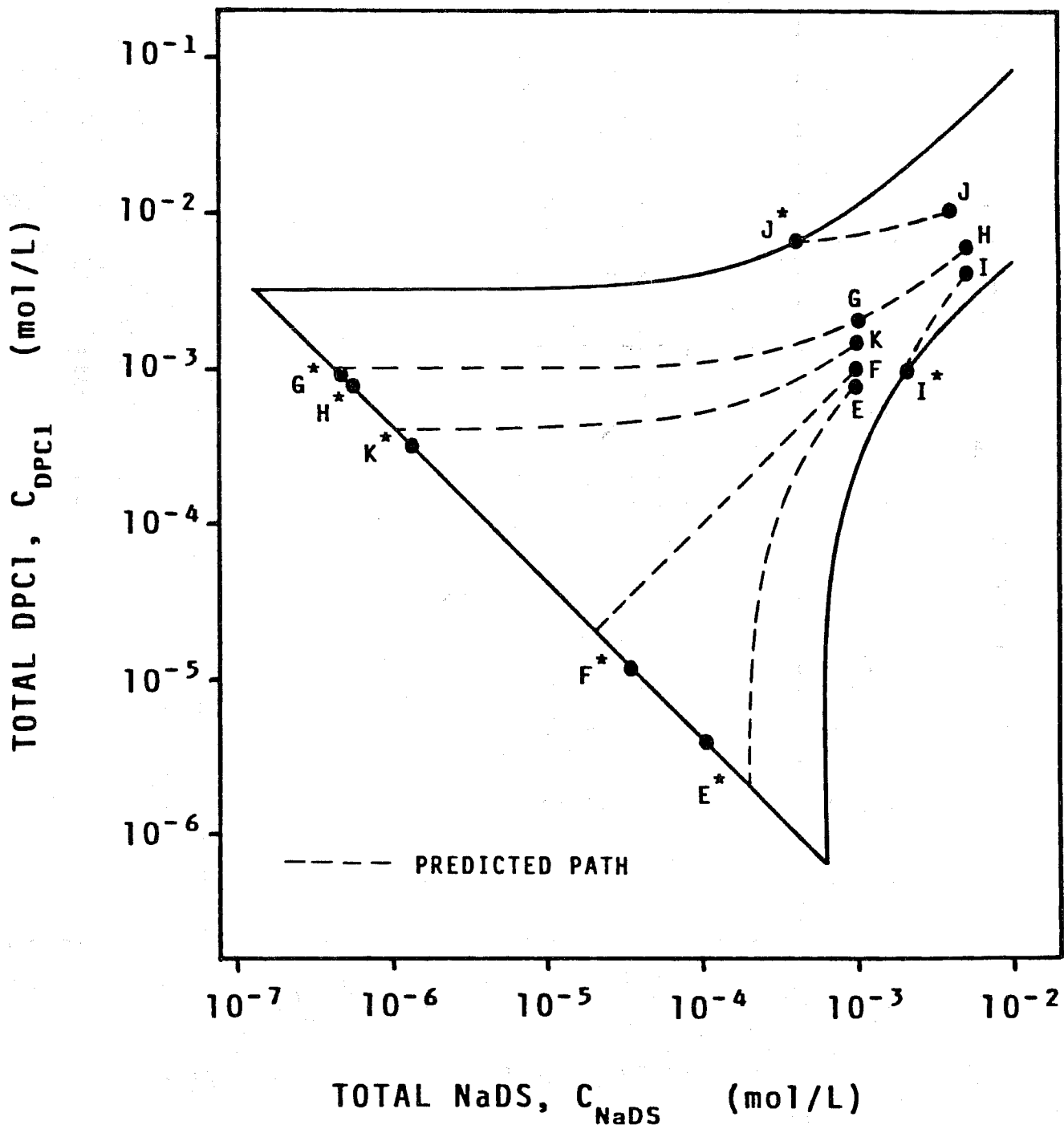


Figure 8. Comparison Between Predicted and Measured Equilibrium Concentrations for Several NaDS-DPCl Mixtures.



CHAPTER 3
THERMODYNAMICS OF ADSORPTION
OF
SURFACTANT MIXTURES ON MINERALS

INTRODUCTION

Surfactant adsorption on mineral oxides has received considerable attention from researchers over the last three decades, including a burst of activity due to the emphasis on surfactant enhanced oil recovery processes in the period since the early 1970's. Relatively little of this work, however, has been focused on systematic studies of the adsorption of well defined mixtures of surfactants on minerals.

Pure component surfactant adsorption on mineral oxides is generally accepted to exhibit a low surface coverage region at low surfactant concentrations which can be described by a Stern-Graham [1], an ion-exchange [2], or a Henry's Law isotherm [3], depending on the counterion concentration [1]. This low coverage region ends abruptly--nearly discontinuously--with a sharp increase in the slope of the isotherm which has long been interpreted as indicating the onset of the formation of local aggregates on the surface. These aggregates have generally been viewed as having very micelle-like properties, and have been referred to as hemimicelles [2] or admicelles [1]. The concentration at which this transition to admicelle formation occurs has been referred to as the Hemimicelle Concentration (HMC) [2] or the Critical Admicelle Concentration (CAC) [1] to emphasize the analogy to the Critical Micelle Concentration (CMC). The CAC has been shown to exhibit the same qualitative dependence on the length [4] and degree of branching [5] of the surfactant hydrophobic moiety as the CMC.

Another major consideration in surfactant adsorption on mineral oxides is the importance of the role of surface heterogeneity in determining the shape of the adsorption isotherm. It has been demonstrated that on a well crystallized substrate the adsorption isotherm consists of a series of observable step changes in coverage, probably corresponding to a transition from low, Henry's Law type

coverage to formation of a complete monolayer or bilayer on a particular crystal face of the adsorbate [6]. This step-wise isotherm corresponds to a surface with a patch-wise distribution in the standard state free-energy change on admicelle formation. When well-crystallized material exhibiting this type of isotherm is mechanically ground, there is an apparent homogenization of the surface, resulting in the formation of many surface patches with values of the standard state free-energy change on admicelle formation intermediate between the values for the patches on the unground material [6].

These considerable analogies between the properties of the surface surfactant aggregate and the bulk solution surfactant aggregate form the basis for the study presented in this paper. Specifically, it is well known that the CMC of mixed surfactant systems can be described by ideal mixing of the pure component micelles when the surfactants are members of a homologous series [7], or by a regular mixing theory (which is analogous to regular solution theory for liquid mixtures) when the surfactant system is composed of a mixture of ionic and nonionic components [7-9]. Mixed micelles composed of ionic and nonionic surfactants exhibit negative deviations from ideality of mixing. In this work, we consider the thermodynamics of mixing in mixed ionic/nonionic admicelles. While previous work has shown that these mixed admicelles show negative deviation from ideal mixing [3], the degree of deviation has not been quantified before now. Since the thermodynamics of mixed ionic/nonionic micelle formation has often been described by regular solution (mixing) theory, we will test the ability of this theory to describe mixed admicelles here.

In a previous paper we applied ideal mixing theory to mixed admicelles of surfactants belonging to a homologous series (sodium decylsulfate and dodecylsulfate) [10]. This work demonstrated that while the concentration at which mixed micelles would form could be well described by ideal mixing, there were significant positive deviations from ideal mixing for the admicelles. We attributed this to the difference in the geometry of the micelle and the geometry of the admicelle and to effects arising from the presence of the surface in the case of the admicelle. For the micelle, its spherical geometry and the highly fluid nature of its core result in ready accommodation of differences in chain lengths. As a result, when a dodecylsulfate ion is incorporated into a decylsulfate micelle, there is a full contribution of the hydrophobic moiety of the dodecylsulfate ion to the free energy of micelle formation; i.e., the activity coefficient is 1 for the longer chain component in the shorter chain component micelle. In the mixed admicelle the hydrophobic moiety of the decylsulfate ion partitioning into a dodecylsulfate admicelle makes a nearly full contribution to the free energy change on mixed admicelle formation. When,

however, a dodecylsulfate ion partitions into a decyl sulfate admicelle, it is not as fully removed from the aqueous solution because of the planar geometry of the admicelle and the relative lack of fluidity of the admicelle, both of which are induced by the presence of the solid surface. Thus, while the mixed micelle exhibits ideal mixing behavior in this system, the mixed admicelle of the same composition exhibits positive deviations from ideal mixing.

It is particularly interesting to apply regular mixing theory to admicelles because it has previously been shown to describe interactions in mixed surfactant aggregates other than micelles, such as monolayers [9] and coacervate [11].

THEORY

For the type of surfactant studied here, at concentrations significantly higher than the CAC, almost all adsorbed surfactant on the surface is in the form of admicelles; i.e., the patches with Henry's Law adsorption contribute an insignificant amount of adsorbed surfactant to the total.

Now consider the pure anionic surfactant adsorption isotherm in this concentration region in Figure 1. At any specific total adsorption level above the CAC, some patches on the surface contain admicelles, with the rest of the surface patches having only sparse coverage of surfactant. The solution concentration at which a specific local patch undergoes transition to admicelle coverage will be referred to as the local patch critical admicelle concentration for the anionic surfactant, CAC^*_A , and is a characteristic of that patch.

For each of the mixture adsorption isotherms, there is also some total adsorption level at which all patches of the same energy level will be covered with admicelles, but patches with lower adsorption energies will only be covered sparsely. The total mixture surfactant concentration at which a local patch will undergo transition to admicelle coverage will be referred to as the local patch mixture critical admicelle concentration, CAC^*_M . By comparing the pure anionic critical admicelle concentration for a particular patch (CAC^*_A) to the mixture critical admicelle concentration (CAC^*_M) of that same surface patch as a function of the composition of the surfactant monomer in solution, it should be possible to determine if the formation of mixed admicelles on that patch is following a regular mixing rule.

The application of a regular mixing rule to mixed micelle formation is now well established. If CMC_A is the critical micelle concentration of the pure anionic surfactant

at the mixture counterion concentration, CMC_N is the critical micelle concentration of the pure nonionic surfactant, and CMC_M is the critical micelle concentration of the mixture, then we obtain the following from regular mixing theory:

$$[f_i x_i / y_i] = [CMC_M / CMC_i]; \quad i = A \text{ or } N \quad [1]$$

$$f_A = \exp\{x_N^2 W / RT\} \quad [2]$$

$$f_N = \exp\{x_A^2 W / RT\} \quad [3]$$

$$y_A + y_N = 1 \quad [4]$$

$$x_A + x_N = 1 \quad [5]$$

where y_i is the mole fraction of surfactant i in the solution monomer, x_i is the mole fraction of surfactant i in the micelle, f_i is the activity coefficient of surfactant i in the micelle, W is the regular mixing interaction parameter, R is the ideal gas law constant, and T is the absolute temperature. All mole fractions are surfactant-only based mole fractions.

These equations can be combined to obtain:

$$CMC_M = x_A CMC_A \exp\{x_N^2 W / RT\} / y_A \quad [6]$$

$$CMC_M = x_N CMC_N \exp\{x_A^2 W / RT\} / y_N \quad [7]$$

We now wish to apply regular mixing to the mixed admicelles by an analogous procedure. Consider a local patch on the surface with a specific pure anionic critical admicelle concentration, CAC_A^* . Let us call this Patch X. There is a solution concentration of surfactant monomer for a surfactant mixture which is in equilibrium with the admicelles on Patch X, just as the monomer is considered to be in equilibrium with the micelles at a monomeric concentration corresponding to the CMC. Therefore, this total monomer concentration, CAC_M^* , is analogous for admicelles to the CMC_M for micelle formation. If mixing between surfactant components follows a regular mixing rule in the admicelle, then on a specific local patch we can write the following:

$$CAC_M^* = z_A CAC_A^* \exp\{z_N^2 W / RT\} / y_A \quad [8]$$

$$CAC_M^* = z_N CAC_N^* \exp\{(z_A^2 - 1) W / RT\} / y_N \quad [9]$$

where z_A is the mole fraction of anionic surfactant in the admicelle and z_N is the mole fraction of nonionic surfactant in the admicelle. CAC_A^* is the monomer concentration in equilibrium with the admicelles on the patch for pure anionic surfactant, and CAC_N^* is a nonionic surfactant concentration corresponding to an infinite dilution standard state for that patch. Equation (9) is not exactly analogous to equation (7)

because of the use of the infinite dilution standard state for the admicelles. The ability of regular mixing theory to describe how CAC_M^* varies with surfactant composition can now be tested for different patches. The degree of nonideality of mixing is indicated by the adjustable interaction parameter, W/RT . When W/RT is zero, the mixing is ideal. When it is negative, there are negative deviations from ideal mixing. This is analogous to fitting mixture CMC data with regular solution theory to obtain an interaction parameter for nonidealities of mixing in micelles. For admicelles, the experimental monomer/admicelle equilibrium compositions can be compared to those predicted by regular mixing theory.

EXPERIMENTAL

MATERIALS.

The sodium dodecylsulfate ($C_{12}SO_4$) was obtained from Fisher Scientific and was purified by double recrystallization from distilled, deionized water and was filtered through a fritted glass filter to remove insoluble impurities.

The nonionic surfactant, IGEPAL CO-660, was furnished by GAF Corporation. IGEPAL CO-660 is an alkylphenol polyoxyethylene nonionic surfactant. The hydrophilic group is polydisperse, with an average ethylene oxide chain composed of 10 ethylene groups, described by a Poisson distribution. It will be referred to by the abbreviation $NP(EO)_{10}$. No impurities were observed in high performance liquid chromatograms.

The adsorbate was a primarily gamma alumina obtained from Degussa, Aluminum Oxide C, with a manufacturer reported BET surface area of 100 m^2 per gram. The mineral was vacuum dried in batches of 50 grams for 4 hours before use.

METHODS.

Adsorption isotherms were run at constant feed molar ratio of $C_{12}SO_4/NP(EO)_{10}$. The feed solution had a pH of 4.25 and a NaCl concentration of 0.15 M. Ten ml of feed solution was added to 0.5 g alumina in a screw type centrifuge tube and centrifuged at 700 RPM for 45 minutes. The tube was then placed in a water bath at 30°C for 4 days, after which the liquid was decanted from the mineral and analyzed. Surfactant concentrations were analyzed using high performance liquid chromatography with a conductivity detector for the anionic surfactant and a variable wavelength UV detector for the nonionic. The solution pH after equilibration was determined using a combination pH electrode.

RESULTS AND DISCUSSION

Mixed Micelle Formation

Values of CMC_M for the two pure surfactants and well defined mixtures thereof are shown in Figure 2. These measurements were made at a high added salt level (swamping electrolyte) so that counterions contributed by the dissolved surfactant were negligible. CMC_M for a regular mixing rule from equations (6) and (7) is also shown. The value of the regular mixing parameter giving the best fit of the CMC_M data was found to be $W/RT = -1.32$. As is usual for such systems [7-9], regular mixing theory describes the CMC_M data very well. The value of W/RT obtained is also typical of these systems.

Mixed Admicelle Formation

Pure component and mixture total adsorption isotherms are shown in Figure 1. The mixtures are at constant surfactant ratio in the feed, but not necessarily in the final equilibrium solution. The concentration on the abscissa is the equilibrium total surfactant concentration. The individual surfactant adsorption isotherms for the pure surfactants and the mixtures are shown in Figures 3 and 4. These experiments were run in the same swamping electrolyte (0.15 M NaCl) as were the CMC_M measurements. As complete bilayer coverage on this alumina was determined from a plateau adsorption isotherm (not reported here) to correspond to an adsorption density of 980 $\mu\text{moles/g}$, the maximum total adsorption obtained corresponds to completion of less than 50% of a monolayer. While at a coverage of about 0.8 $\mu\text{moles/g}$ the pure $C_{12}SO_4$ isotherm exhibits the expected sharp increase in isotherm slope interpreted as corresponding to the onset of admicelle formation on the surface, it appears that the pure nonionic isotherm reaches the nonionic CMC before pure nonionic admicelles begin to form on the surface. This is why an infinite dilution standard state was chosen for the nonionic surfactant.

Although for adsorption of monoisomeric surfactants in swamping electrolyte it is generally observed that the adsorption reaches a plateau at the CMC, for this system it can be seen that the adsorption of the $C_{12}SO_4$ approximately doubles above the CMC over the region studied. At the low surface coverages studied here, the adsorption appears to be an extremely sensitive function of surfactant chemical potential; therefore, small changes in the chemical potential with total concentration above the CMC, contrary to the constant chemical potential predicted from the pseudo-phase separation model, may account for the change in adsorption above the CMC. Note that the total adsorption isotherm with the steepest slope above the CAC is the one which corresponds

to the 50:50 feed composition isotherm. It is very nearly vertical from a total adsorption of $<1 \mu\text{moles/g}$ to nearly $20 \mu\text{moles/g}$.

The degree of nonideality of this system can be appreciated by observing that while it is questionable whether any pure nonionic admicelles form on adsorption from the pure nonionic feed, addition of only 20% anionic surfactant to the feed results in formation of surface aggregates which are 75% nonionic.

In order to test regular mixing theory for this system, we wish to consider surfactant interactions on a specific patch on the surface over a range of monomer compositions. To do this, it is initially assumed that when the total surfactant adsorption is at the same level on two different isotherms that adsorption is occurring on the same patch, and that patches with lower adsorption energies are only sparsely covered (in the Henry's Law region). For a specific surfactant mixture, the total surfactant monomer concentration in the solution corresponding to this adsorption level is called CAC_M^* . Since we know both the mole fraction of monomer for each component in the solution as well as the mole fraction of each component in the admicelle, we can solve equations (6) and (7) directly for the necessary value of W/RT at the chosen adsorption level on each isotherm. Values of CAC_M^* were obtained by extrapolation of data obtained at low y_M to a y_M of unity [12]. The calculational procedure selected was the following:

1. Select a total adsorption level from the pure anionic adsorption isotherm on Figure 1.
2. Select a mixture isotherm on Figure 1.
3. Read CAC_M^* and y_A from Figure 1.
4. Use equations (6) and (7) to calculate both z_A and W/RT necessary for a regular mixing rule to be followed.

The results for cuts at both the $2 \mu\text{mole/g}$ level and the $6 \mu\text{mole/g}$ level are summarized in Table 1. At the $2 \mu\text{mole/g}$ adsorption level W/RT varies from $+1.19$ for $z_A=0.56$ to -2.92 for $z_A=0.34$. At the $6 \mu\text{mole/g}$ level W/RT varies from $+0.90$ for $z_A=0.70$ to -5.35 for $z_A=0.54$. If regular mixing theory described the variation of z_A with y_A , then W/RT should be independent of z_A . Instead we observe W/RT to be a strong function of z_A , though the observed W/RT as a function of y_A is a smooth, monotonically decreasing function.

As an alternate approach, let us assume that regular mixing theory does describe the admicelle, and then choose a method for fixing the interaction parameter. Two methods of fixing the interaction parameter which suggest themselves are: (1) to use the value of W/RT obtained from fitting CMC_M , and

(2) to fit equations (6) and (7) to the y_A and CAC_M^* values obtained from the mixture isotherms. The first method yields $W/RT = -1.32$; the second method yields a value that is dependent on the adsorption level at which we read the isotherms. Having fixed W/RT we can then calculate z_A and CAC_M^* for the y_A of each mixture isotherm at the total adsorption level of the pure component isotherm and compare them to the experimental values of z_A and CAC_M^* .

Comparisons of the theoretical and experimental values are presented in Figures 5-8. The W/RT giving the best fit of CAC_M^* at the 2 $\mu\text{mole/g}$ level is -0.787 ; the best fit at the 6 $\mu\text{mole/g}$ level is -1.34 . In Figures 5 and 6, the predicted CAC_M^* values differ grossly from the experimental data.

Figures 7-8 present the theoretical and experimental values of z_A at different monomer compositions. While the qualitative trend of the curves is more nearly correct in this comparison, the numerical values again show gross differences between theory and experiment. It might appear that by adjusting the value of W/RT , the theoretical curves could be made to satisfy both the CAC_M^* values and the z_A values. In fact, if W/RT is adjusted to improve the fit to one variable, the fit to the other deteriorates.

To avoid confusion, it is worthwhile to point out the reason that the theoretical CAC_M^* curves obtained here have a different shape from those usually seen in applying regular mixing theory to mixed surfactant CMCs. It is because for the mixed admicelle system there is no experimentally obtainable pure nonionic CAC_N^* to be used in the equations to "anchor" the low anionic mole fraction end of the curve. Essentially, the theoretical curve is approaching a hypothetical pure component nonionic critical admicelle concentration on the local patch which may be obtained by extrapolating from the infinite dilution nonionic standard state CAC_N^* . The theoretical curves can be made to show a minimum by making W/RT more negative, but this results in an even poorer fit of the CAC_M^* data at high anionic mole fractions in Figures 5-6 and also results in even worse fits of the admicelle composition data shown in Figures 7-8.

It should also be noted from Figures 7-8 that an azeotrope is observed experimentally at both adsorption levels. The regular mixing curves do predict the existence of azeotropes for the systems, but they are, again, badly wrong in composition. In both cases the experimental azeotrope composition corresponds to approximately a 50:50 mole ratio of anionic/nonionic in both the monomer phase and the admicellar phase. In fact, for equilibrium concentrations that varied from very low concentrations to concentrations well above the mixture CMC, it was observed that a 50:50 feed composition resulted in almost equimolar

adsorption of the components. These observations seem to suggest that minimization of the electrostatic contribution to the free energy of the aggregates is a dominating force in determining the composition of the admicelles, and that this is not accounted for in the regular mixing theory.

This particular test would tend to indicate that regular mixing theory is completely inadequate to describe the mixing of anionic and nonionic admicelles. A serious objection to this conclusion, however, is the assumption that the admicelles exhibit ideal areas of mixing. In fact, given the assumed mechanism for the large negative deviations from ideality observed in micelles and monolayers, we would expect that the area/mole of the two components would be a function of the composition of the admicelle. It is possible, then, that we are not comparing admicelles on the same surface patch when we compare compositions at the same total adsorption.

An alternate method of applying regular mixing theory to the system to account for the above problem is to (1) assume a value for W/RT , for example from the mixed micelle results, (2) select a mixture isotherm, (3) determine the value of y_A which is approximately constant for that isotherm, then (4) use equations (6) and (7) to calculate CAC_M^* . The point on the mixture isotherm corresponding to the correct value of CAC_M^* then gives an experimental value of the total adsorption for the same fraction of the surface as was covered on the pure component isotherm if regular mixing theory is correct. The results of following this procedure are illustrated in Figure 9 and tabulated in Table 2. The solid lines in Figure 9 connect the points on the mixture isotherms which have values of y_A and CAC_M^* which satisfy the regular mixing relations. As can be seen from Table 2, the μ moles of surfactant per gram of adsorbent at constant fractional coverage is predicted to vary by over an order of magnitude. At the 2 μ mole/g level, the adsorption density at which the chosen patch undergoes transition to admicelle formation varies from 0.24 μ moles/g at an anionic surfactant monomer mole fraction of 0.13, to 4.6 μ moles/g at an anionic monomer mole fraction of 0.47. Similarly, for the patch corresponding to formation of a pure anionic admicelle at a coverage of 6.0 μ moles/g, the adsorption density at which this patch undergoes transition to admicelle formation increases to 9.8 μ moles/g at an anionic monomer mole fraction of 0.99 and to 17.7 μ moles/g at an anionic monomer mole fraction of 0.94. If this were correct it would correspond to a factor of 3 increase in the number of moles/area over a 0.06 change in mole fraction. These results are physically unreasonable.

OBSERVATIONS AND CONCLUSIONS

While regular mixing theory can predict the CMC and micellar composition for mixed ionic/nonionic micelles, it does not appear to be able to accurately describe mixed ionic/nonionic admicelles. The thermodynamic assumptions behind regular mixing theory have been shown [7] to be incorrect for mixed micelles. It is a coincidence that it describes mixed micelle behavior so well. It is not surprising, therefore, that it does not properly describe mixed admicelle behavior. Better thermodynamic models to describe mixing of surfactant aggregates of various types are badly needed. At present the most promising approach seems to be explicitly dealing with the electrostatic interactions within the aggregates.

REFERENCES

1. Harwell, J.H.; Hoskins, J.C.; Schechter, R.S.; Wade, W.H. Langmuir, 1985, 1, 251.
2. Somasundaran, P.; Fuerstenau, D.W. J. Phys. Chem., 1964, 70, 90.
3. Scamehorn, J.F.; Schechter, R.S.; Wade, W.H. J. Colloid Interface Sci., 1982, 85, 463.
4. Wakamatsu, T.; Fuerstenau, D.W. Advan. Chem. Ser. 1968, 79, 161.
5. Dick, S.G.; Fuerstenau, D.W. J. Colloid Interface Sci. 1971, 37, 595.
6. Goujon, G.; Cases, J.M.; Mutaftschiev, B. J. Colloid Interface Sci. 1976, 56, 587.
7. Scamehorn, J.F., in "Phenomena in Mixed Surfactant Systems," J.F. Scamehorn, editor, ACS Symp. Ser. 1986, 311, 1.
8. Holland, P.M. Adv. Colloid Interface Sci., in press.
9. Rosen, M.J. in "Phenomena in Mixed Surfactant Systems," J.F. Scamehorn, editor, ACS Symp. Ser., 1986, 311, 144.
10. Roberts, B.L., Scamehorn, J.F., Harwell, J.H., in "Phenomena in Mixed Surfactant Systems," J.F. Scamehorn, editor, ACS Symp. Ser., 1986, 311, 200.
11. Yoesting, O.E., Scamehorn, J.F. Colloid Polym. Sci. in press.

TABLE 1

EFFECT OF ADMICELLE COMPOSITION ON REGULAR SOLUTION
INTERACTION PARAMETER AT CONSTANT TOTAL ADSORPTION

Mole Fraction Anionic Surfactant in Admicelle	W/RT
<u>Total Adsorption = 2 μmoles/g</u>	
0.56	+1.19
0.46	-0.09
0.45	-0.92
0.30	-1.19
0.34	-2.92
<u>Total Adsorption = 6 μmoles/g</u>	
0.70	+0.90
0.48	-0.07
0.42	-0.75
0.30	-1.43
0.54	-5.35

TABLE 2

ADSORPTION LEVELS AT THE PREDICTED ANIONIC MOLE FRACTION
OF SURFACTANT MONOMER FROM REGULAR MIXING THEORY

W/RT = -1.32 (from mixture CMC data)

Anionic mole fraction surfactant monomer	Adsorption (μ moles/g)
---------------------------------------------	--------------------------------

2 μ mole/g Pure Anionic Surfactant Adsorption

0.13	0.24
0.47	4.6
0.79	5.0
0.90	6.0
0.98	3.9
1.0	2.0

6 μ mole/g Pure Anionic Surfactant Adsorption

0.13	0.24
0.50	4.8
0.85	11.5
0.94	17.7
0.99	9.8
1.0	6.0

Figure 1. Effect of Feed Composition on Total Adsorption from $C_{12}SO_4$ and $NP(EO)_{10}$ Mixtures on Alumina.

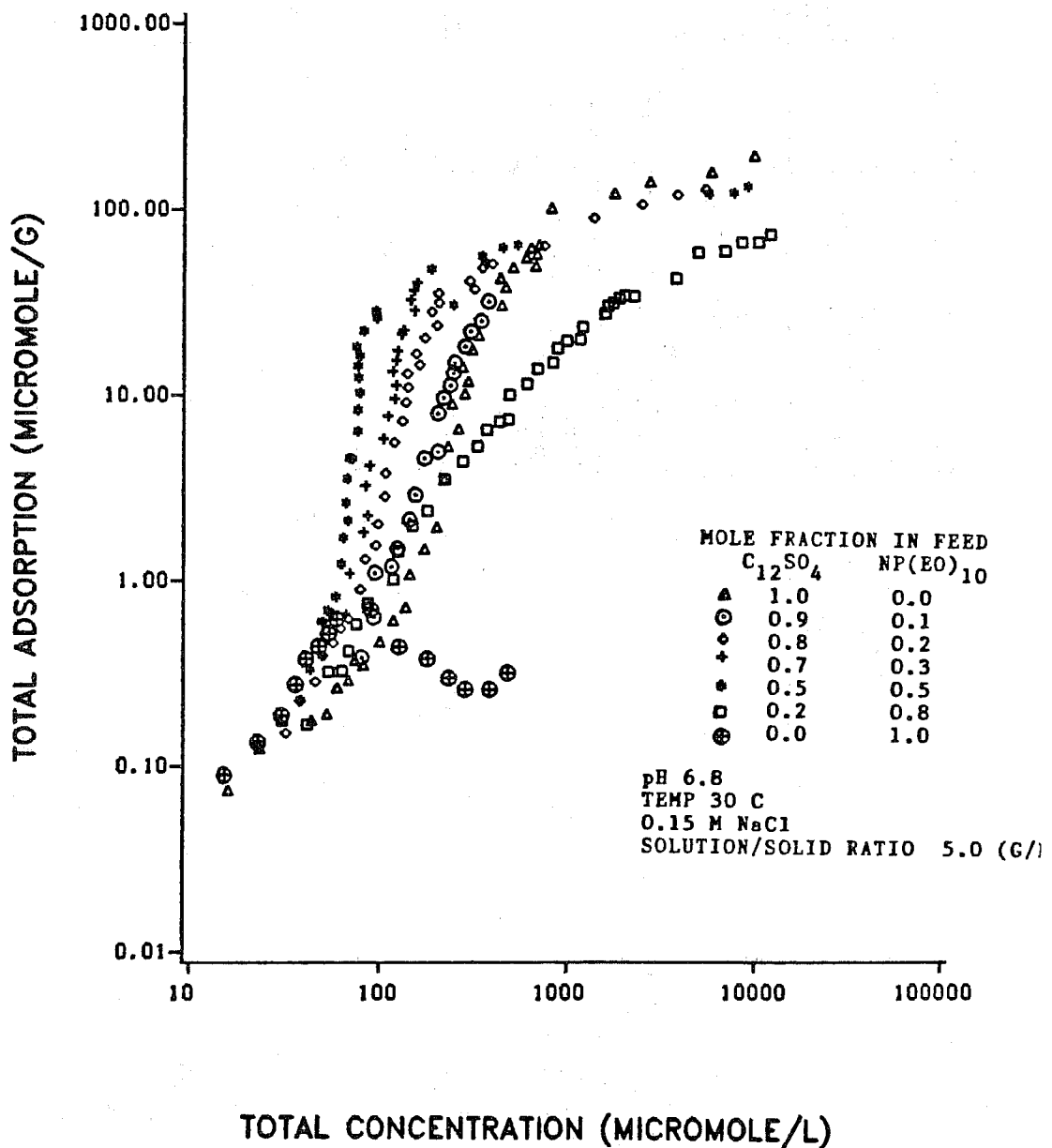


Figure 2. Regular Solution Theory Fit of Mixture CMC Data for $C_{12}SO_4/NP(EO)_{10}$.

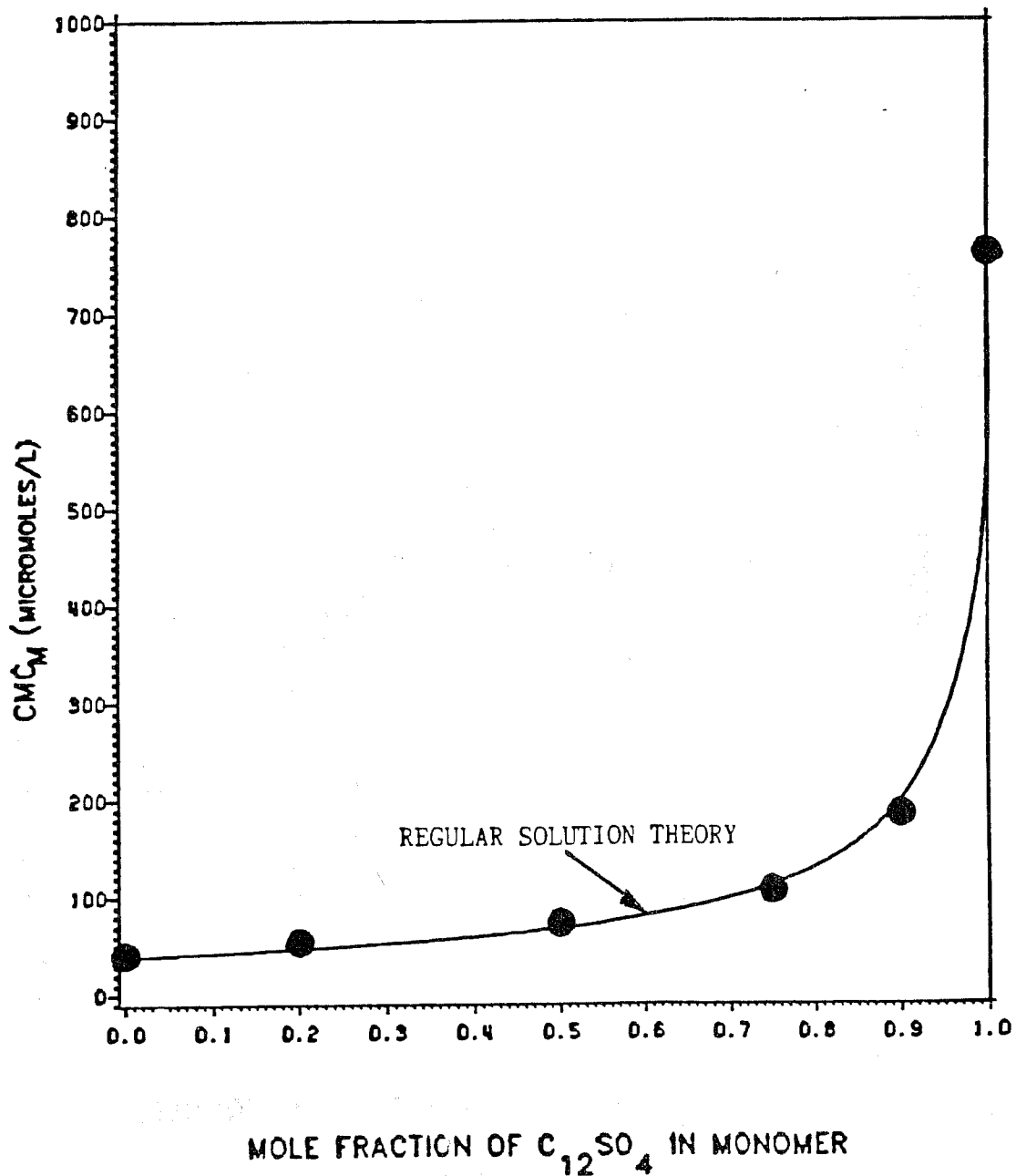


Figure 3. Effect of Feed Composition on $C_{12}SO_4$ Adsorption from $C_{12}SO_4$ and NP(EO)₁₀ Mixtures on Alumina.

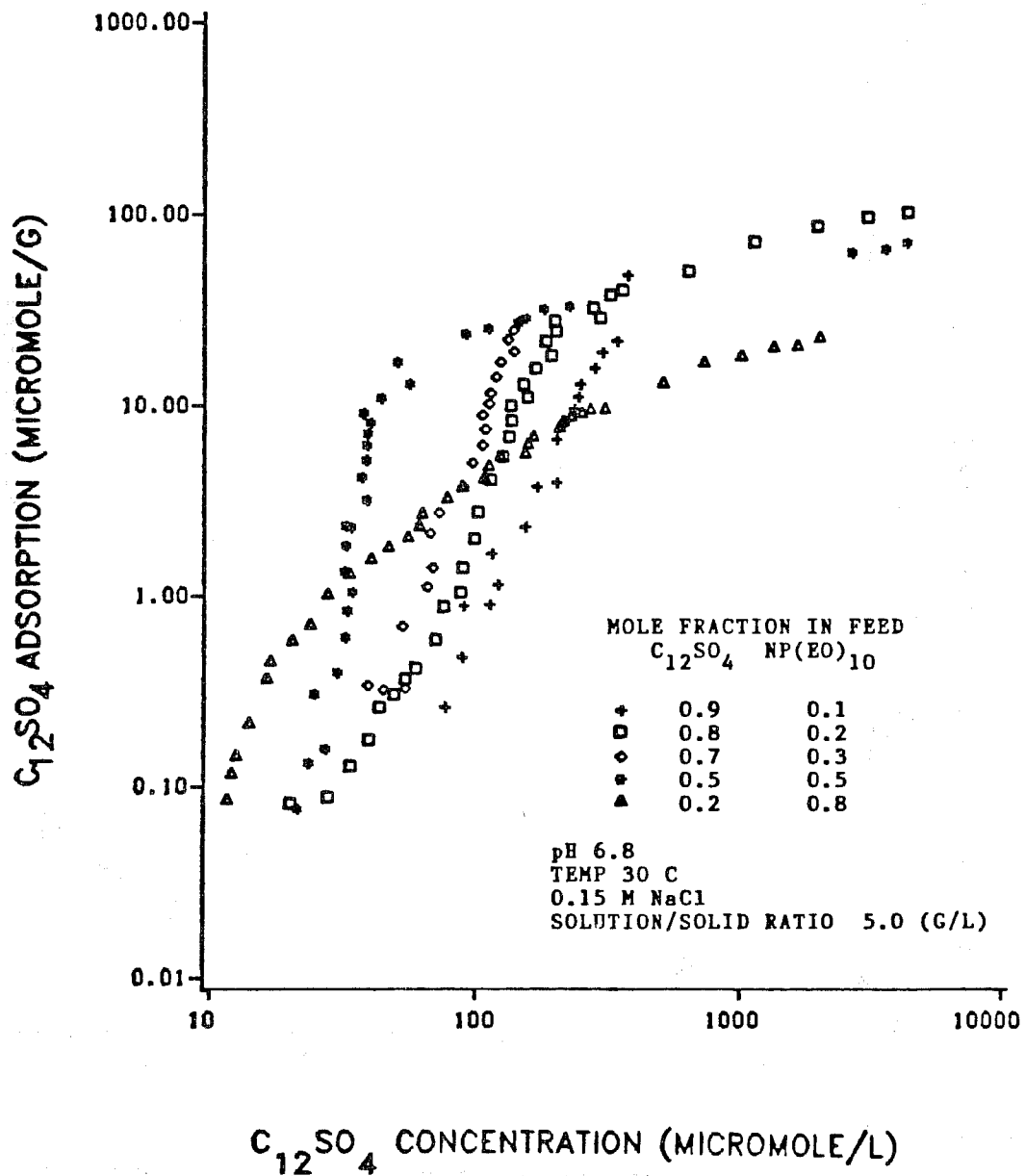


Figure 4. Effect of Feed Composition on NP(EO)₁₀ Adsorption from C₁₂SO₄ and NP(EO)₁₀ Mixtures on Alumina.

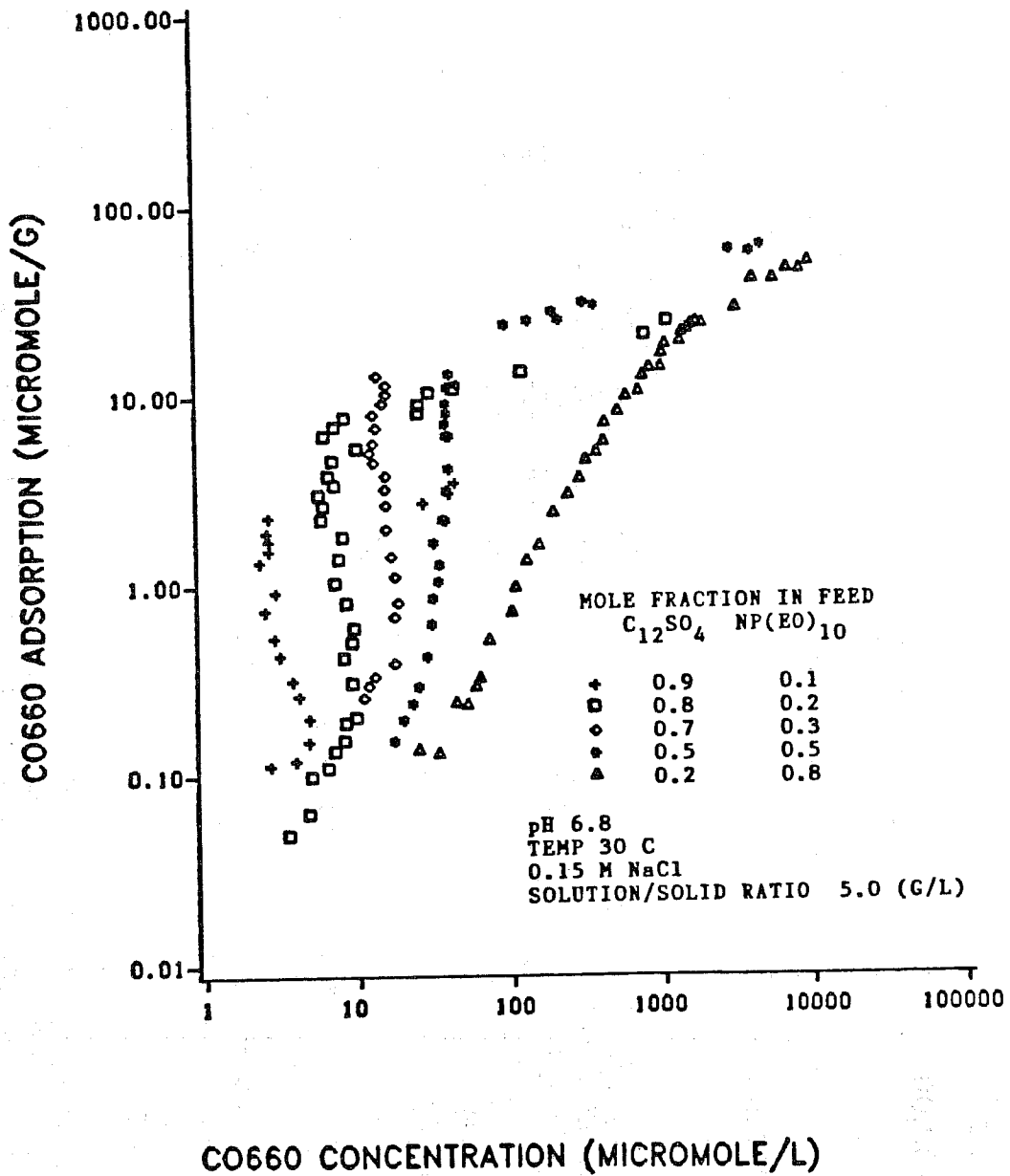


Figure 5. Regular Solution Fit of Patch CAC_M^* Data at the 2 Micromoles/g Adsorption Level.

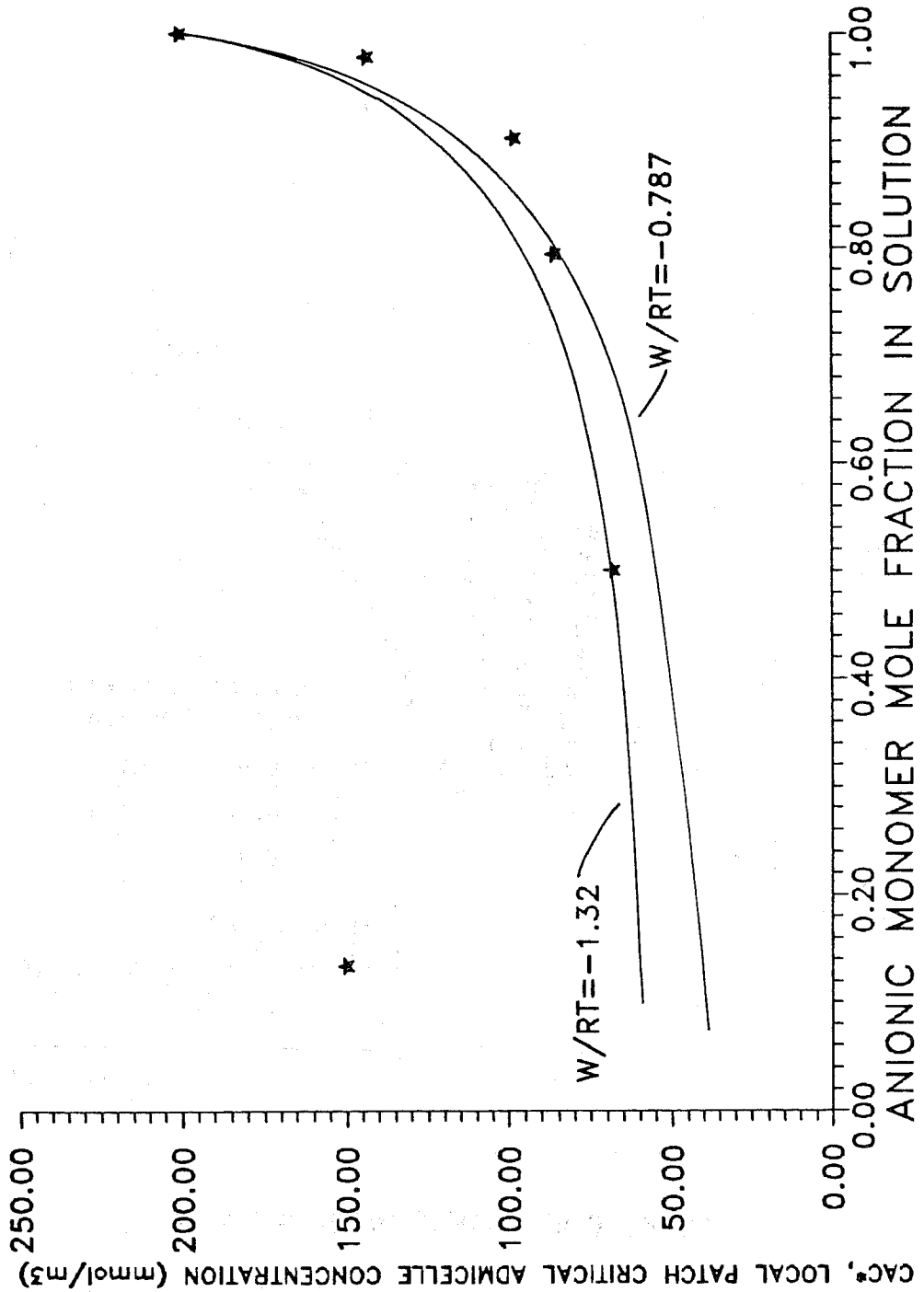


Figure 6. Regular Solution fit of Patch CAC_M^* Data at the 6 Micromole/g Adsorption Level.

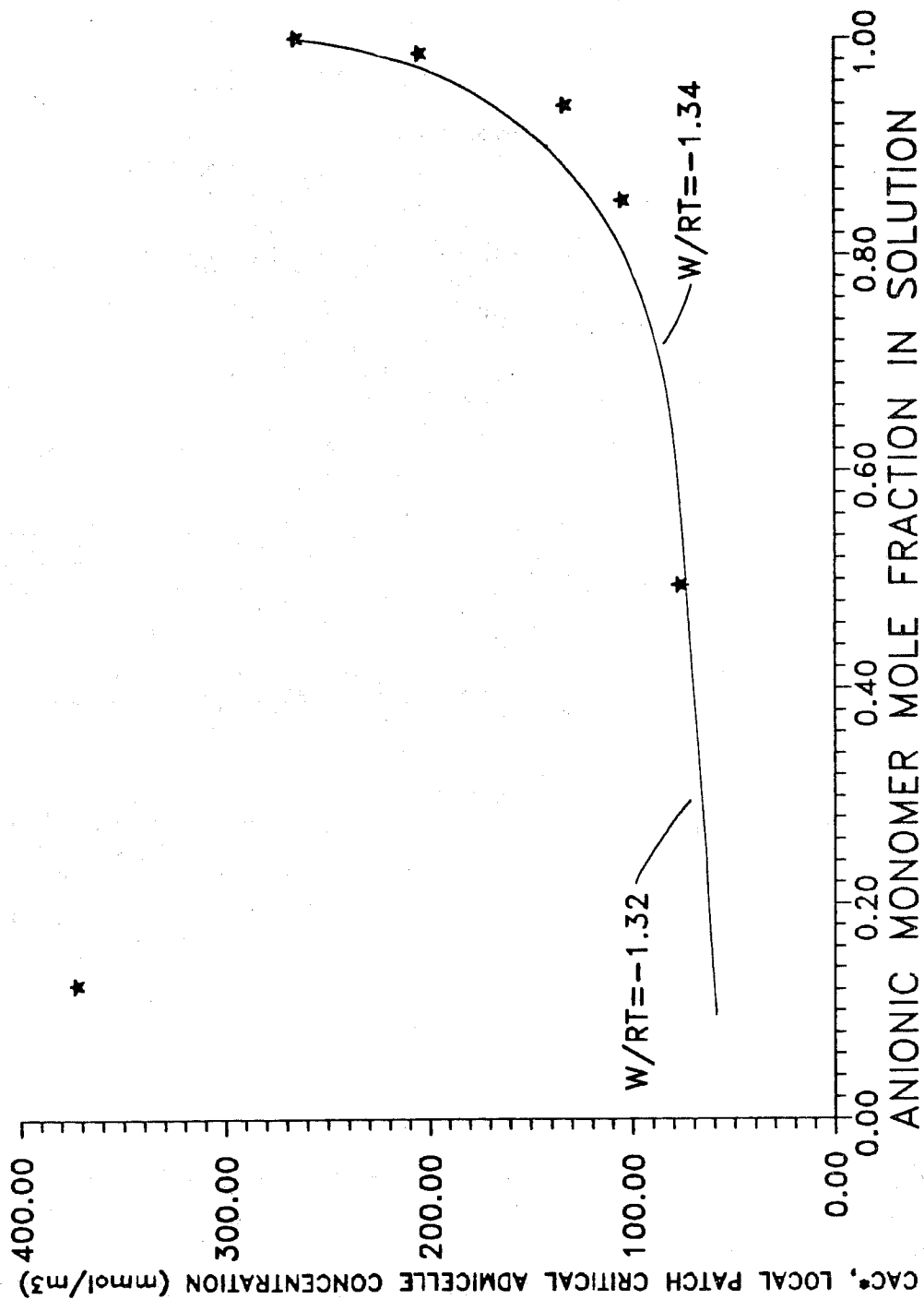


Figure 7. Regular Solution Fit of Admicelle Mole Fraction Data at the 2 micromole/g Adsorption Level

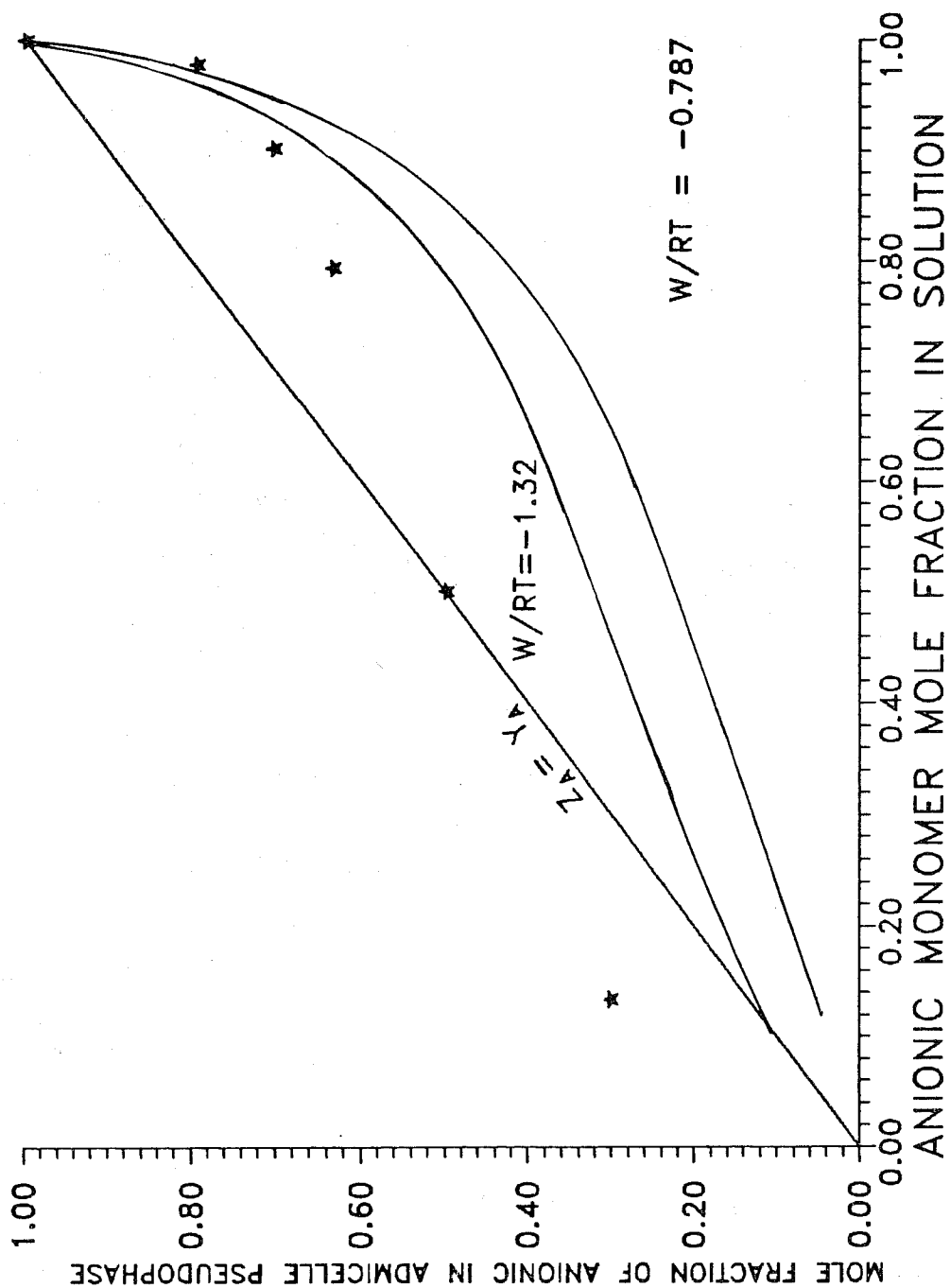


Figure 8. Regular solution Fit of Admicelle Mole Fraction Data at the 6 micromole/g Adsorption Level

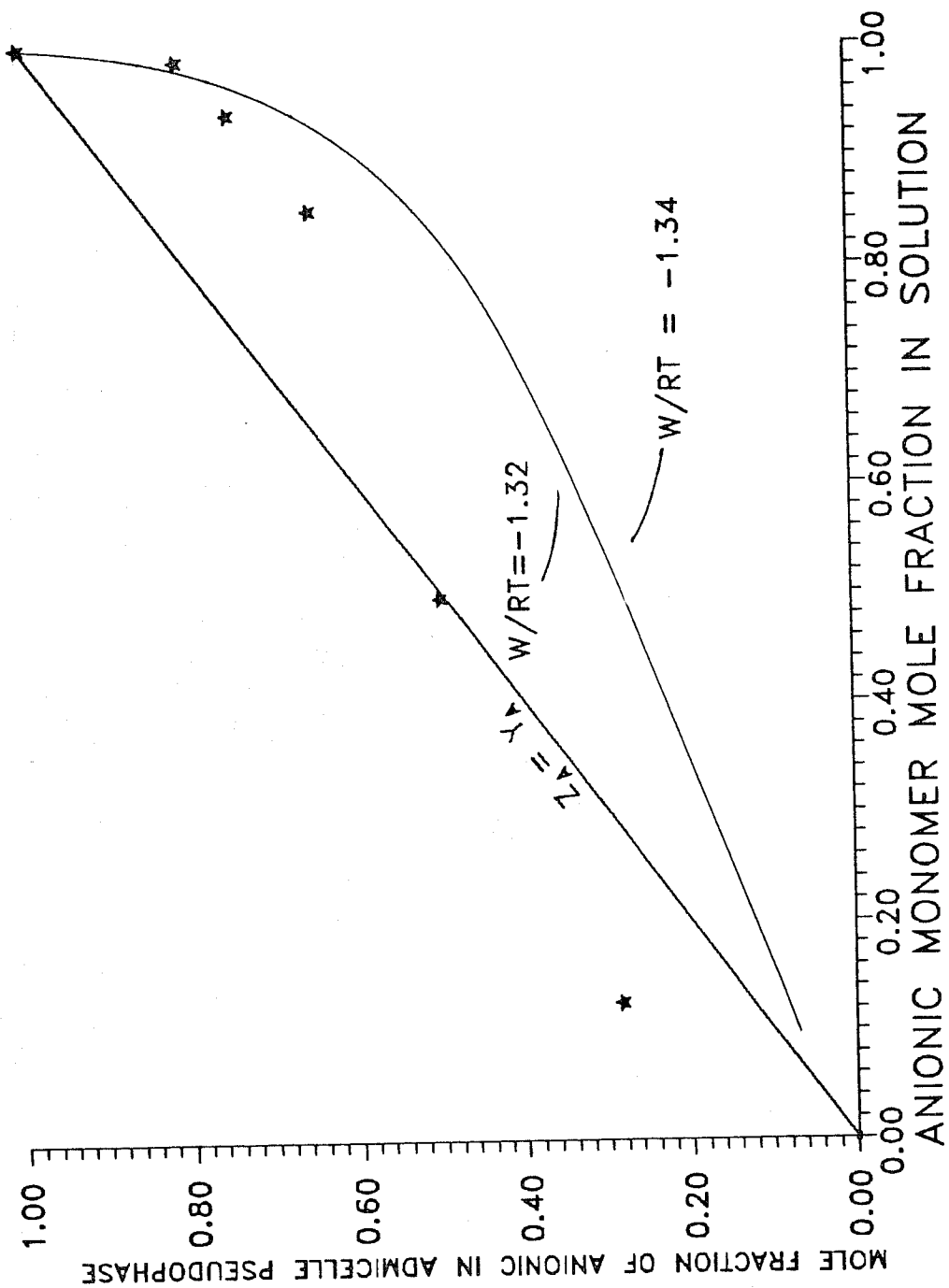
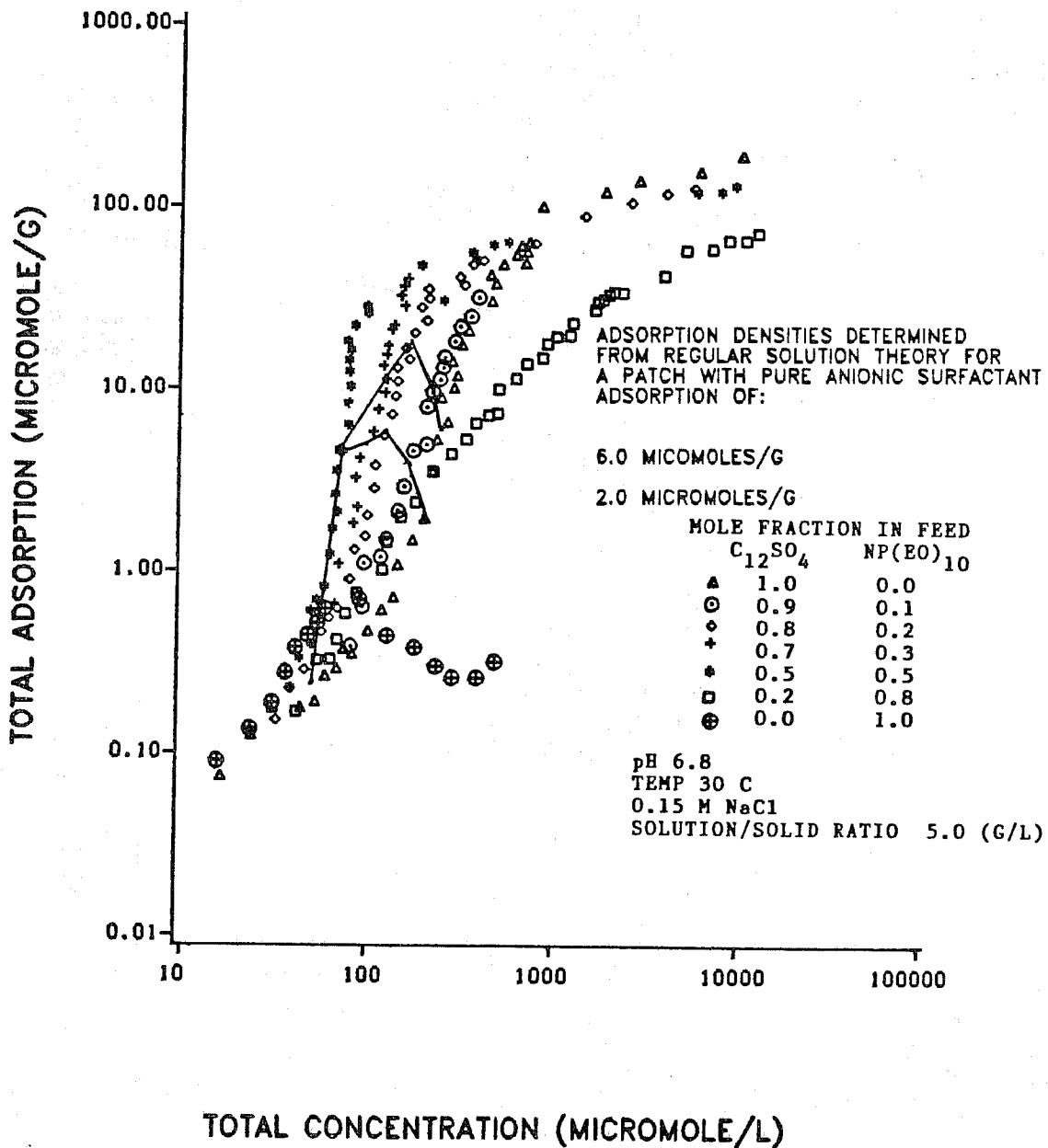


Figure 9. Predicted Adsorption Densities from Regular Solution Theory.



CHAPTER 4

SANDPACK STUDIES

The new process we are proposing here depends on two physical phenomena: 1) The chromatographic movement of dilute surfactant solutions [7,8] and 2) the occurrence of spontaneous phase separations from dilute surfactant solutions with the addition of a small amount of another appropriately selected surfactant [9].

When a concentration change of an adsorbing component in a dilute solution is propagated through a porous medium, the velocity of the concentration change will be less than the velocity of the carrier fluid. For example, when an aqueous surfactant solution is injected into a sandpack, some of the surfactant molecules will adsorb out of the solution and onto the minerals of the sandpack. Any particular individual surfactant molecule will spend part of its time on the immobile solid surface and part of its time in the mobile bulk solution. When it is in the mobile phase the surfactant molecule is carried along at the velocity of the mobile phase, but when it is on the solid surface it is immobile and has a velocity of zero. This gives each molecule of surfactant, and thereby the change in surfactant concentration itself, an effective velocity which is less than that of the velocity of the mobile phase. The greater the equilibrium adsorption of the surfactant species from the solution, the greater the fraction of its total time in the sandpack each surfactant molecule will spend on the immobile solid surface and the the lower effective velocity of the surfactant concentration change relative to the velocity of the mobile phase. If, for example, an aqueous slug of surfactant is injected into a sandpack, and the surfactant adsorbs on the minerals of the sandpack, then the velocity of the surfactant slug will be less than the bulk fluid velocity, even though the surfactant is contained completely within the aqueous phase and the surface of the solid with which the aqueous phase is in contact. If we change the structure of the surfactant molecule so that it spends less time on the solid surface and more time in the moving fluid phase, i.e. if we reduce its equilibrium adsorption from the solution, then a slug of that surfactant will have a greater chromatographic velocity. Conversely, if we change its structure so that it spends more time immobile on the solid surface and less time in the moving aqueous phase, i.e. if we increase its equilibrium adsorption, then we will reduce its chromatographic velocity.

This phenomenon is represented schematically in Figure 1. In Figure 1.a we show a dilute solution of surfactant being injected into a sandpack (or core), and make the assumption that the mobile aqueous phase is in local equilibrium with the solid phase (the distribution of surfactant molecules between the solution and the surface is the same as if they were in a test tube together). The front of the surfactant slug will be sharp [1,2], the concentration of surfactant behind the slug front will be the same as the injected concentration, and the velocity of the slug front is given by a simple mass balance across the slug front [1]:

$$\frac{V_{\text{FRONT}}}{V_{\text{BULK FLUID}}} = \frac{1}{1 + \frac{\Gamma_{\text{CMC}}}{C_{\text{INJ}}}} \quad [1]$$

In this expression, V_{FRONT} is the velocity of the front of the surfactant slug, $V_{\text{BULK FLUID}}$ is the velocity of the bulk fluid (or, equivalently, of a non-adsorbing tracer), C_{INJ} is the concentration of the surfactant in the slug as it is being injected, and if the solution contains micelles then Γ_{CMC} is the adsorption onto the mineral from a solution of the surfactant at a concentration above its Critical Micelle Concentration (CMC) in units of moles per unit volume of the porous medium. Note from this equation that as the adsorption at the injected concentration is increased, the velocity of the slug front is decreased. When we begin to inject brine behind the surfactant slug, if the concentration of the surfactant in the slug is above the surfactant's CMC, so that the solution contains micelles, then two new "concentration waves", i.e. propagationally stable variations in surfactant concentration, begin to move through the sandpack. The wave labeled "REAR" in Figure 1.b is a concentration wave of variation between the injected composition downstream and a region of surfactant at its CMC upstream. The velocity of this wave is the same as the velocity of the bulk fluid, since it is just a variation of micelle concentration at constant monomer concentration and constant surfactant adsorption [1]. Wave "REAR" will then be a sharp concentration variation; i.e., it will occur over a narrow fraction of the sandpacks total length. The wave labeled "TAIL" in Figure 1.b is a wave of concentration variation between the region at the surfactant's CMC and a region containing only brine with no surfactant at all. Depending on the shape of the surfactant's adsorption isotherm, wave "TAIL" may or may not be a sharp variation in concentration [2]. Its velocity can be approximated by the following expression [1]:

$$\frac{V_{\text{TAIL}}}{V_{\text{BULK FLUID}}} = \frac{1}{1 + \frac{\Gamma_{\text{CMC}}}{\text{CMC}}} \quad [2]$$

(All the variables in equation 2 are defined analogously to those in equation 1.) After brine has been injected behind the surfactant slug for some period of time, there will be a growing region near the injection point that has no surfactant in it, either on the solid surface or in the bulk solution. If a second surfactant slug is then injected into the same sandpack, the velocity with which its front will propagate into the sandpack will also be given by equation [1]. If we want the second surfactant slug to overtake the first one, then we just must make sure that 1) the velocity of the front of the second slug is greater than the velocity of the tail of the first slug, and that 2) we do not give the first slug too great a head start. Equations [1] and [2] show us the variables which can be manipulated to obtain this situation: CMCs, plateau adsorptions (i.e. the adsorption above the CMC, which will be approximately constant for a monoisomeric surfactant), slug volumes, and brine spacer volume.

It is possible, then, to inject a slug of a surfactant into an adsorbing medium, follow it by injected brine--free of surfactant--for some almost arbitrary period of time, then inject a surfactant with a greater chromatographic velocity and have the second surfactant slug overtake the first, slower moving slug inside the porous medium. It is important to note that the in situ mixing of the two slugs does not require the mixing of two different fluid phases within the porous medium, as both surfactants are within the same aqueous phase; rather, this "mixing" actually consists of the interpenetration of two concentration waves within a single phase. It can be pictured as the molecules of the second surfactant, which by design spend less time on the surface of the solid phase than those of the first surfactant, catching up with and then "leap frogging" the molecules of the first surfactant within the same moving aqueous phase. There should be no concern, then, about any inability of the process to achieve in situ mixing of fluids of different viscosities or different densities, as this is not what takes place. It is actually more accurate to think of the interaction of the two surfactant slugs not as a mixing process, but rather as the interference of two waves moving within the same medium.

If the two surfactants in the two different slugs have been chosen so that on mixing they will undergo a phase change, then on the interpenetration of the front of the fast slug with the tail of the slow slug, an equilibrium surfactant phase can be made to separate from the solution in situ. If the surfactant phase which separates from the solution is capable of blocking the pore throats within the porous medium, then the flow path which the slugs have

followed will become sealed off to any subsequently injected fluids. Two surfactant phases which suggest themselves as possibly useful for blocking the region in which this slug interpenetration occurs are the solid precipitate phase and the viscous, gel-like coacervate phase [3] which surfactants are known to form. The same combination of two surfactant species can in general form either of these two potentially interesting phases, depending upon their concentrations in the region where mixing occurs. Since the phases formed are in thermodynamic equilibrium with the solutions from which they separated, they can be expected to be stable over periods of time long relative to the time of an enhanced recovery process. In dilute solutions surfactant phase separations also occur very slowly, taking periods of up to several weeks to occur under laboratory conditions. If achieved in situ, this phenomenon would allow deep interpenetration of the slugs before the flow path of the fluid was changed by plug formation, so that the plugs themselves, once fully formed, could fill significant portions of the flow paths.

A unique aspect of this surfactant enhanced volumetric sweep efficiency process is that the distance from the injection point at which the front of the fast surfactant slug overtakes the tail of the slow surfactant slug can be either very large or very small, depending on the relative velocities of the two concentration waves which first interact and the size of the brine "spacer" injected between the two surfactant slugs. This can be illustrated more clearly by the use of distance/time diagrams [1]. In Figure 2.a the trajectories of the waves shown in Figure 1 are plotted along with the trajectories of the waves generated by the injection of the second surfactant slug.

In order to make the illustration more concrete, we will assume that the surfactants being used are the anionic surfactant sodium dodecylsulfate (SDS) and the cationic surfactant cetyl pyridinium chloride (CPC), and that the sand pack consists of a bed of alumina powder. While SDS is unsuitable for reservoir applications because of the susceptibility of sulfates to hydrolysis at reservoir temperatures, and while CPC probably has too high a molecular weight to be propagated a suitable distance away from the well bore in a reasonable length of time, these two compounds are commercially available in monoisomeric form and exhibit behavior analogous to that which would be required of compounds suitable for an actual reservoir treatment.

In Figure 2.a the ordinate is the distance a concentration wave has travelled from the injection point, and the abscissa is the total number of pore volumes of the continuous mobile phase which have been injected since the beginning of the injection of the first surfactant slug. The slopes of the wave trajectories are then the chromatographic velocities

of the concentration variations induced by the injection of the slugs. Note that along the abscissa the volumes of the SDS slug, the brine spacer, and the CPC slug are indicated. Because the alumina in the sand pack has a positive surface charge, the anionic surfactant will have the lowest chromatographic velocity in this system, and so should be injected first. The CPC, having the same charge as the mineral surface, and so being repelled by the surface, will have the higher velocity, and so should be the surfactant of the second slug. Starting from the vertical axis of the plot, the first trajectory is, then, the trajectory of the front of the SDS slug, the second is that of the slug rear (which travels at the bulk fluid velocity and so has a chromatographic velocity of 1.0), and the third is that of the tail of the SDS slug. During the injection of the brine space, all of these waves propagate away from the injection point. When the CPC slug is injected, the front of the CPC slug moves at very nearly the bulk fluid velocity, since the CPC has a very low adsorption on alumina. When the front of the CPC slug overtakes the tail of the SDS slug, either a solid precipitate phase or a viscous coacervate phase will separate from the mobile aqueous phase, plugging the sand pack. The distance above the abscissa at which the SDS tail and the CPC front interact is the distance from the injection point at which plugging first occurs, and is indicated on the distance/time diagram by the distance A.

In Figure 2.b the same injection sequence is represented, but now the size of the brine spacer has been increased. Now the SDS tail is further from the injection point when CPC injection begins, and the distance from the injection point at which the phase separation begins to occur will be greater, as indicated by the relative size of the lengths A and B indicated on the diagrams in Figure 2.

No one even cursorily acquainted with the complexities of real reservoirs and of the materials with which such a process would have to be made to work would fail to realize that though the above description is conceptually simple, substantial research will need to be done to establish the feasibility of the process for field testing. Though many aspects of the process will have to be examined before such a test could be designed, some of the first questions which might be asked are whether a dilute surfactant solution could produce enough precipitate or coacervate to plug a core or pack, whether the surfactant slugs would show sufficient preference for the higher permeability regions of a core or pack for plugging to be selective, and whether even a simple system could produce a tertiary recovery of oil under laboratory conditions. Experimental results presented below will address these questions.

EXPERIMENTAL

Two different surfactants were used in this work. An anionic surfactant, sodium dodecyl sulfate (SDS), and a cationic surfactant, cetyl pyridinium chloride (CPC). The chemical structures of these surfactants are shown in figure 3. The SDS was a Kodak Laboratory Chemicals product and was recrystallized from ethanol before use. The CPC, a gift from Hexcel Chemical Products, was food grade and was used as received. Both surfactants exhibited only one peak upon HPLC analysis. The sand packs consisted of standard glass preparative liquid chromatography columns dry-packed with alpha-aluminum oxides obtained from ALFA PRODUCTS. Two aluminas of different particle sizes were used to produce packs of different permeabilities. The low surface area ($\approx 3 \text{ m}^2/\text{g}$) alumina had particle sizes of 1-15 micron. The high surface area ($\approx 320 \text{ m}^2/\text{g}$) alumina had a particle size of 40 microns and was porous.

All solutions contained 0.15M NaCl. Deionized, distilled water was used to make the brine solution. All surfactant solutions were made by first weighing the surfactant for a certain concentration and then adding the salt solution to bring the solution to the desired concentration; 0.1 M HCl was used to adjust the pH of all solutions to pH = 4. The NaCl and HCl were reagent grade.

Three sets of static measurements were performed on the surfactant solutions: (1) surface tension measurements in order to measure the value of the CMC of the surfactants, (2) phase boundaries in order to find the limits of different regions for the mixed surfactant system used in this study, (3) individual surfactant adsorption isotherms in order to measure the extent of surfactant adsorptions on the mineral oxide. The determination of the CMC was made by standard procedures using a ring tensiometer. For the phase boundary determinations, after the mixtures of SDS and CPC at different concentrations reached equilibrium (after a period of 3 to 4 weeks), they were visually checked for any traces of precipitate or coacervate. The equilibrium concentrations of SDS and CPC in the equilibrated supernatant of the solutions, which of necessity fell on the phase boundaries, were measured by use of high pressure liquid chromatography (HPLC) with a Tracor 951A chromatographic pump and Bausch & Lomb Spectronic 1001 spectrophotometer (at 260nm wavelength) respectively. A column packed with reverse phase silica gel was used in the HPLC system. By changing the carrier fluid from water to 50/50 water and methanol, SDS was first separated from the NaCl in the system and then flushed from the column into the conductivity cell of the Wescan 201A conductivity detector of the HPLC. The detailed procedure for the use of HPLC and the results of the static experiments are reported elsewhere [4].

Two series of flow experiments were conducted in oil

free systems in the second part of the work: (1) single column runs to show that permeability of a sand pack can be reduced by the mechanism proposed and (2) double column runs in order to show the selectivity of plugging in higher permeability zones. To demonstrate the ability of the process to produce a tertiary recovery of oil from a sand pack, parallel columns, one packed with each of the two aluminas used in the study, were first saturated with n-heptane, then waterflooded to produce a residual oil saturation. Details of the experimental set-up and procedure are available elsewhere [4]. The parameters monitored in the flow experiments were the pressure drop across the bed or beds, flow rate from each column used, and the fluid levels in the feed burets, except for the single column study reported, which was run before pressure monitoring equipment could be attached to the system.

RESULTS AND DISCUSSION

Experimental conditions for the flow experiments are summarized in Table 1. In the single column experiments performed, injection of a dilute solution of the anionic surfactant (SDS), was followed by a brine slug, and then injection of a dilute solution of the cationic surfactant (CPC). In general, flow rate reductions of 15% to 50% were achieved.

The results of experiment 1, a single column run, are reported in Figure 4, and the experimental parameters in Table 2. The column porosity, based on a mass balance, was 82.1%, and the void volume (or pore volume, pv) was 1.28 ml. Eleven pore volumes of the standard brine were injected through the column before the beginning of the measurements shown in Figure 4. Through-out injection of the brine preflush, a uniform flow rate of 0.092 ml/min was observed. One pore volume (1.28 ml) of SDS at its critical micelle concentration (800 moles/l or 230 parts per million) was injected into the column at the beginning of the period reported in the Figure 4. This was followed by 1/2 pore volume of brine and 1/2 pore volume of CPC at 20 times its critical micelle concentration (640 moles/l or 220 ppm). The flow rate remained approximately constant until 80 minutes into the run (the slight increase in flow rate after two pore volumes appears to have been due to the need to shut off the pump in the original experimental set up when changing the injected solution); at this time the flow rate began an exponential decrease which continued until the run was terminated after three hours. During the progress of the run, channeling was observed to be occurring between the bed and the column wall at two points, one in the middle of the column and one nearer the end of the column. It would seem that these should be associated with regions of plug formation. From the injected concentrations and compositions surfactant precipitation would be expected. The overall flow

rate declined 34%; permeability reduction was probably much greater, as it appeared that pressure built up until channeling between the bed and the wall was observed, which was not seen before surfactant injection had occurred. This would correspond to forcing the flowing fluids into the low permeability regions of a reservoir. Additionally, continued flushing with brine resulted in the disappearance of the channels, apparently through partial dissolution of the plugs. The flow rate, however, was not observed to substantially recover even after the apparent channeling disappeared.

The results of experiment 2, a parallel sand pack run, are shown in Figure 5, which is a plot of the flow rate through each column versus the cumulative pore volumes injected, and the experimental parameters are summarized in Table 3. As in the preceding experiment, only results following the initial brine preflush are plotted in the figure. Initially, 69% of the flow was through column 1. As mentioned before, the fluctuation in flow rate during injection of surfactants and brine spacer appears to be due to slight differences in the pump setting following the switching of feeds. During injection of the brine drive after the last surfactant slug, the flow rate through column 1, the higher permeability column, started to decrease, falling to 0.001 ml/min after 17.3 pv had been injected. It remained almost constant at this value, which was below the flow rate through the low permeability column, column 2, until the end of the run. Up to 16 pv after injection of the CPC slug the percentage of the flow going through the high permeability column remained high (between 60% and 90% of the overall flow through the parallel packs), but it then decreased, dropping to only 30% of the total flow during the last 4 pv before the run was terminated. It can be speculated from this that the precipitate was fully formed only after the time required for the 16 pv to be injected, and this resulted in final attainment of a stable flow condition. It should be recalled that in the static experiments several weeks were often needed before any precipitate fully formed. The primary result of significance from this run is the demonstration of preferential or selective plugging, even though 30% of the flow was already going through the low permeability column before the process began.

A similar injection sequence was repeated with the two parallel sandpicks in experiment 3, but now with both originally filled with n-heptane and then water flooded, in parallel, so that both had the same pressure drop, until secondary production ceased. The results are plotted in Figure 6 and the experimental parameters are shown in Table 4. The two different particle size powders of alpha-alumina were used so that the porosity and permeability of the two sandpicks differed. The high and low permeability columns were saturated with n-heptane to 57% oil saturation and 82%

oil saturation, respectively. During the waterflood, 42% of the oil initially in the high permeability column (18% of the oil initially in place, OIIP) was recovered. During this step all 100% of the flow was passing through column 1, so that no oil was recovered from column 2. The surfactant injection sequence resulted in complete blockage of the high permeability sandpack, so that 100% of the flow was diverted into the low permeability column, resulting in recovery of an additional 35% of the original oil in the low permeability column. Continued flushing with brine resulted in an increase in the flow rate through column 1. This was probably due to partial dissolution of the plugs. As is evident from Figure 6, however, the flow rate through the high permeability column still did not substantially recover.

CONCLUSIONS

The following conclusions are suggested by the experimental reported here:

1. By using the phase behavior and chromatographic movement of surfactants, formation of plugs in a porous medium can be achieved using very dilute solutions of surfactants.
2. The high permeability regions of a sand pack can be selectively plugged by in situ mixing of sequentially injected surfactants resulting in a surfactant phase separation.
3. An enhanced oil recovery by surfactant enhanced volumetric sweep efficiency after normal water flooding can be achieved in sand packs of significant permeability variation.

NOMENCLATURE

C_{INJ}	the concentration of surfactant in a slug as it is being injected, moles/ M^3 of medium
CMC	Critical Micelle Concentration (CMC) of a surfactant, moles/ M^3 of medium
E_D	displacement efficiency, fractional residual oil in place/ M^3 of medium contacted by displacing fluid
E_R	the oil recovery efficiency of the water-flooding process, fractional residual oil in place/ M^3 of medium
E_V	volumetric sweep efficiency, fraction of medium contacted by injected fluids
$V_{\text{BULK FLUID}}$	linear velocity of the bulk fluid, M/s
V_{FRONT}	linear velocity of the front of the surfactant slug, M/s
V_{TAIL}	linear velocity of the tail of the surfactant slug, M/s

Greek Letters

Γ_{CMC}	surfactant adsorption onto the mineral from a solution of the surfactant at a concentration above its CMC, moles/ M^3 of medium
-----------------------	-----------------------------------------------------------------------------------------------------------------------------------

REFERENCES

1. J.H. Harwell, F.G. Helfferich, and R.S. Schechter, "Effect of Micelle Formation on Chromatographic Movement of Surfactant Mixture," AICHEJ., 28 (3), 448, 1982.
2. J. H. Harwell, R. S. Schechter, and W. H. Wade, "Surfactant Chromatographic Movement: An Experimental Study," AICHE Journal, 31, (3), 415, 1985.
3. E. Tomlinson, S.S. Davis and G.I. Mukhayer, "Ionic Interaction and Phase Stabilities," Solution Chemistry of Surfactants, Vol. I., p. 3, K.L. Mittal, Ed., Plenum Press, New York, 1979.
4. Arshad, Alireza, "Enhanced Oil Recovery by Surfactant Enhanced Volumetric Sweep Efficiency," M.S. Thesis, The University of Oklahoma, School of Chemical Engineering and Materials Science, May 1985.

TABLE 1

EXPERIMENTAL CONDITIONS IN FLOW EXPERIMENTS

COLUMN LENGTH (cm) - 15

COLUMN CROSS
SECTIONAL AREA (cm²) - 0.0707

COLUMN VOLUME (cm³) - 1.0603

CRITICAL MICELLE CONCENTRATION IN
STANDARD BRINE (.15 M NaCl):

SDS - 830 μ M (830 mmols/m³)

CPC - 33 μ M (33 mmols/m³)

ADSORPTION OF SURFACTANT ON MINERAL
ABOVE CMC:

ON 1-15 MICROMETER ALUMINA

SDS - 23.0 mmols/Kg

CPC - 0.35 mmols/Kg

ON 40 MICROMETER ALUMINA

SDS - 84.0 mmols/Kg

CPC - 0.56 mmols/Kg

TABLE 2

SYSTEM PARAMETERS, EXPERIMENT 1

PREFLUSH	- 11.0 PORE VOLUMES (pv)
VOLUME OF SDS SLUG	- 1.00 pv
VOLUME OF BRINE SPACER	- 0.50 pv
VOLUME OF CPC SLUG	- 0.50 pv
VOLUME OF BRINE DRIVE	- 10.4 pv
COLUMN PORE VOLUME	- 1.28 cm ³
STEADY STATE FLOW RATE AT END OF PREFLUSH	- 0.092 ml/min (1.53 x 10 ⁻³ cm ³ /s)
POROSITY OF SAND PACK	- 0.821
SURFACTANT CONCENTRATIONS IN SLUGS:	
SDS	- 830 μM (830 mmol/m ³)
CPC	- 660 μM (660 mmol/m ³)

TABLE 3

SYSTEM PARAMETERS, EXPERIMENT 2

PREFLUSH	- 1.7 PORE VOLUMES (pv)
SDS SLUG VOLUME	- 0.38 pv
CONCENTRATION	- 3320 mmol/m ³
BRINE SPACER VOLUME	- 1.25 pv
CPC SLUG VOLUME	- 0.37 pv
CONCENTRATION	- 3300 mmol/m ³
BRINE DRIVE VOLUME	- 16.5 pv

	COLUMN 1	COLUMN 2
INITIAL FLOW RATE (cm ³ /S)	3.71 x 10 ⁻⁴	1.61 X 10 ⁻⁴
PORE VOLUME (cm ³)	0.86	0.79
POROSITY	0.81	0.74
PER CENT OF TOTAL FLOW		
INITIAL	68.9	31.1
FINAL	50.8	49.2

TABLE 4

SYSTEM PARAMETERS, EXPERIMENT 3

PREFLUSH	- 1.0 PORE VOLUMES (pv)
SDS SLUG VOLUME	- 0.6 pv
CONCENTRATION	- 24900 mmol/m ³
BRINE SPACER VOLUME	- 2.0 pv
CPC SLUG VOLUME	- 0.6 pv
CONCENTRATION	- 3300 mmol/m ³
BRINE DRIVE VOLUME	- 8.0 pv

	COLUMN 1	COLUMN 2
PORE VOLUME (cm ³)	0.833	0.783
PER CENT OF TOTAL OIL RECOVERED:		
FROM WATERFLOOD	42%	0%
BY SURFACTANT ENHANCED VOLUMETRIC SWEEP EFFICIENCY	0%	31%

Figure 1. Injection of a dilute surfactant slug.

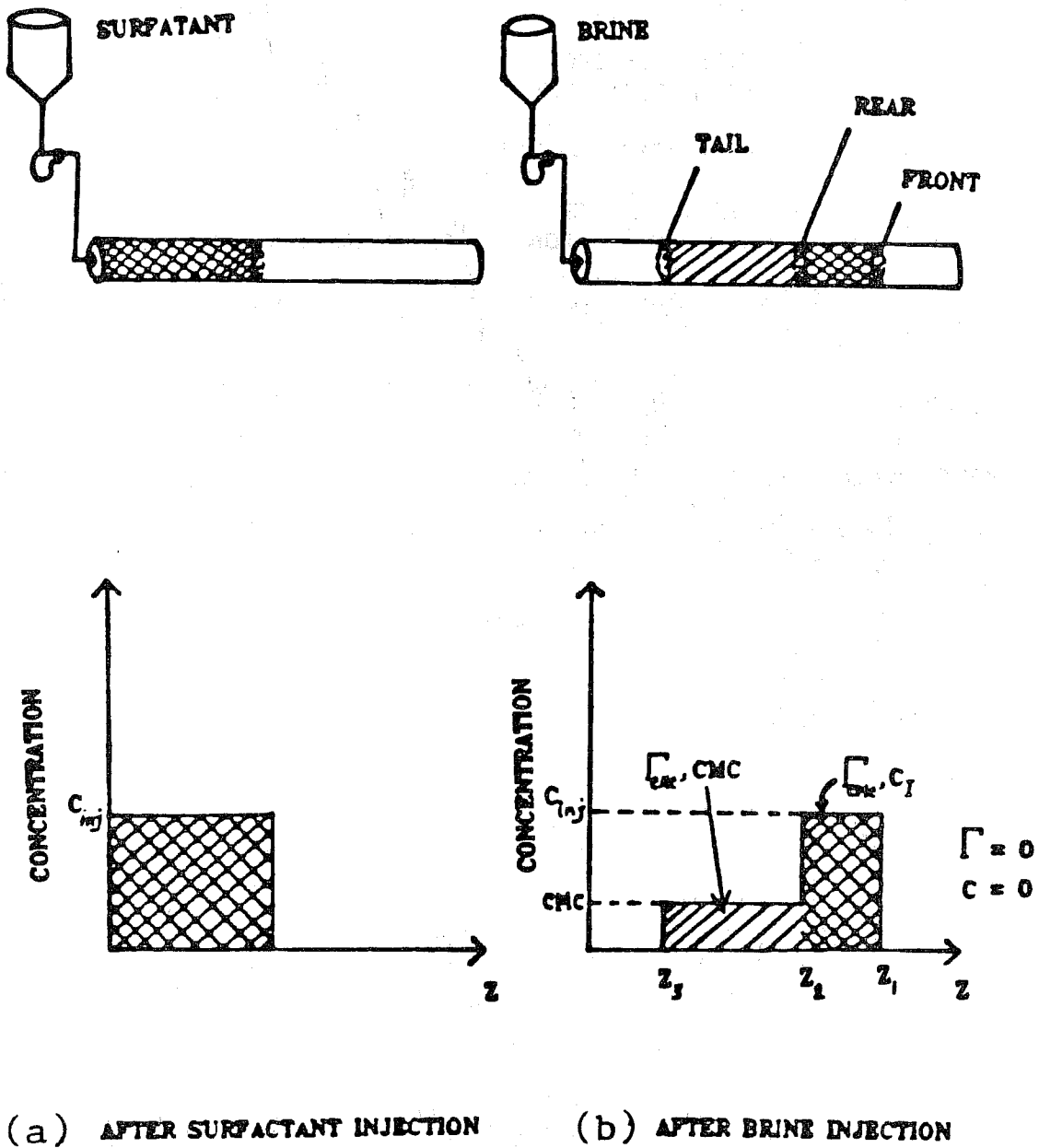
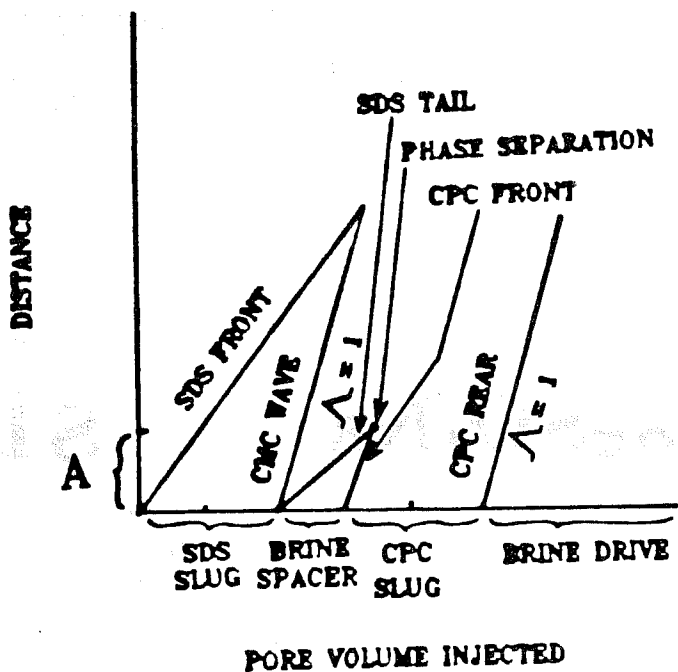


Figure 2. Interaction of two dilute surfactant slugs separated by a brine spacer.



(a)

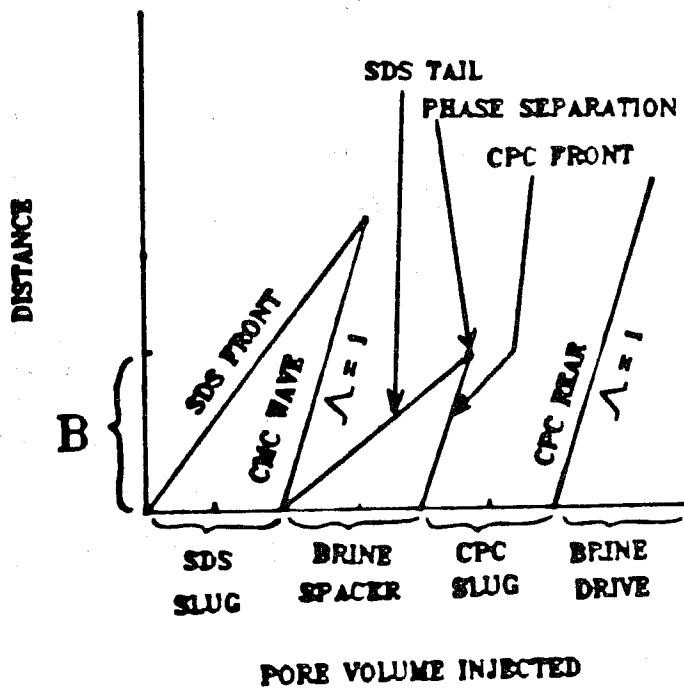


Figure 3. Chemical structures of surfactant used in experiments reported in this chapter.

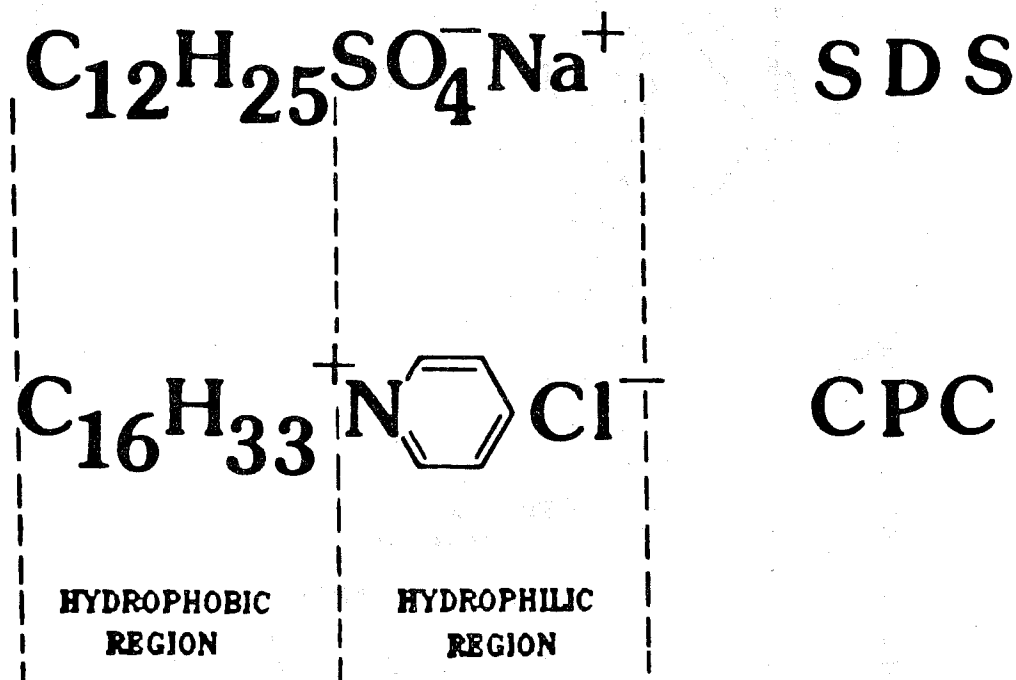


Figure 4. Sandpack plugging by dilute surfactants.

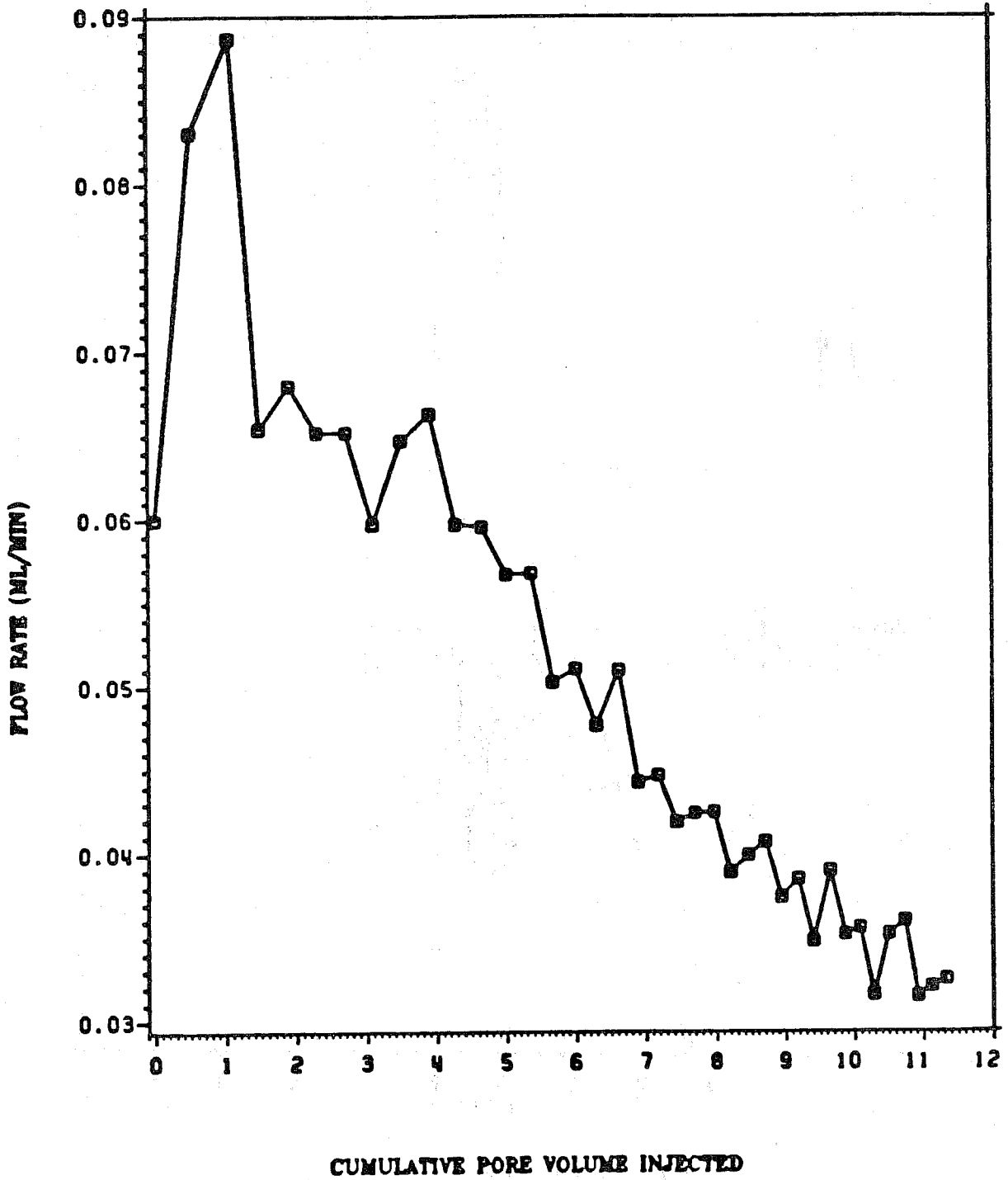


Figure 5. Selective plugging of high-permeability sand pack.

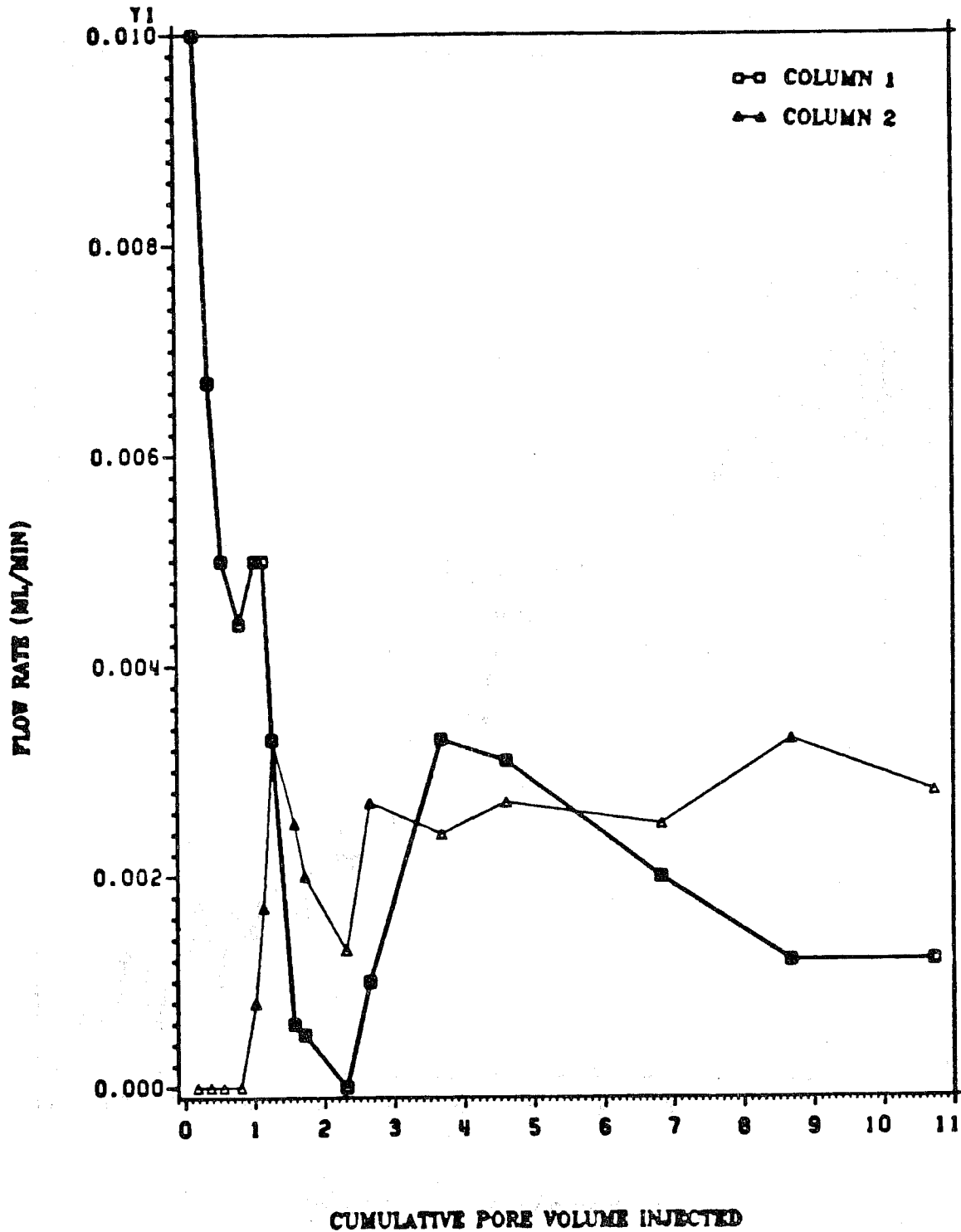


Figure 6. Tertiary production from low-permeability sand pack.

